AFWAL-TR-85-4124

ADA104O6U

ADVANCES IN THE STUDY OF THE
MECHANICAL BEHAVIOR OF MATERIALS

N. E. Ashbaugh
M. Khobaib
T. Weerasooriya
G. A. Hartman
A. M. Rajendran
D. C. Maxwell
R. C. Goodman

UNIVERSITY OF DAYTON
RESEARCH INSTITUTE
300 COLLEGE PARK DRIVE
DAYTON, OHIO   45469
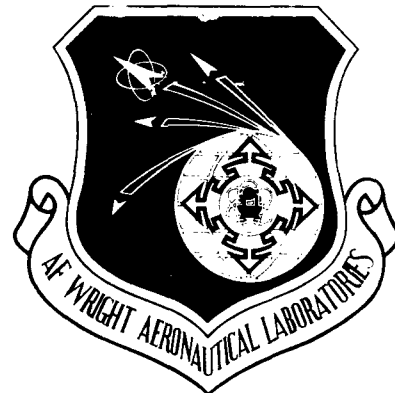
DECEMBER 1985   **Best Available Copy**

FINAL REPORT FOR PERIOD COVERING 15 JUNE 1981 - 30 SEPTEMBER 1984

APPROVED FOR PUBLIC RELEASE; DISTRIBUTION UNLIMITED

MATERIALS LABORATORY
AIR FORCE WRIGHT AERONAUTICAL LABORATORIES
AIR FORCE SYSTEMS COMMAND
WRIGHT-PATTERSON AIR FORCE BASE, OHIO   45433

20040218348

This technical report has been reviewed and is approved for publication.

THEODORE NICHOLAS, Project Engineer
Metals Behavior Branch
Metals and Ceramics Division
Materials Laboratory

ALLAN W. GUNDERSON, Tech Area Mgr
Metals Behavior Branch
Metals and Ceramics Division
Materials Laboratory

FOR THE COMMANDER
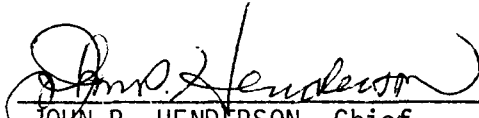
JOHN P. HENDERSON, Chief
Metals Behavior Branch
Metals and Ceramics Division
Materials Laboratory

REPORT DOCUMENTATION PAGE

1a. REPORT SECURITY CLASSIFICATION Unclassified		1b. RESTRICTIVE MARKINGS		
2a. SECURITY CLASSIFICATION AUTHORITY		3. DISTRIBUTION/AVAILABILITY OF REPORT Approved for Public Release; Distribution Unlimited		
2b. DECLASSIFICATION/DOWNGRADING SCHEDULE				
4. PERFORMING ORGANIZATION REPORT NUMBER(S)		5. MONITORING ORGANIZATION REPORT NUMBER(S) AFWAL-TR-85-4124		
6a. NAME OF PERFORMING ORGANIZATION University of Dayton Research Institute	6b. OFFICE SYMBOL (If applicable)	7a. NAME OF MONITORING ORGANIZATION Materials Laboratory AFWAL/MLLN		
6c. ADDRESS (City, State and ZIP Code) 300 College Park Drive Dayton, Ohio 45469		7b. ADDRESS (City, State and ZIP Code) Air Force Wright Aeronautical Labs. Wright-Patterson AFB, Ohio 45433		
8a. NAME OF FUNDING/SPONSORING ORGANIZATION Materials Laboratory	8b. OFFICE SYMBOL (If applicable) AFWAL/MLLN	9. PROCUREMENT INSTRUMENT IDENTIFICATION NUMBER F33615-81-C-5015		

8c. ADDRESS (City, State and ZIP Code) Wright-Patterson AFB, Ohio 45433	10. SOURCE OF FUNDING NOS.			
	PROGRAM ELEMENT NO.	PROJECT NO.	TASK NO.	WORK UNIT NO.
11. TITLE (Include Security Classification) ADVANCES IN THE STUDY OF THE MECHANICAL BEHAVIOR OF MATERIALS	61102F	2307	P1	14

12. PERSONAL AUTHOR(S) N. E. Ashbaugh, M. Khobaib, T. Weerasooriya, G. A. Hartman, D. C. Maxwell, A. M. Rajendran, R. C. Goodman				
13a. TYPE OF REPORT Final	13b. TIME COVERED FROM 6/81 TO 8/84	14. DATE OF REPORT (Yr., Mo., Day) December 1985		15. PAGE COUNT 134

16. SUPPLEMENTARY NOTATION

17.	COSATI CODES		18. SUBJECT TERMS (Continue on reverse if necessary and identify by block number)
FIELD	GROUP	SUB. GR.	Crack growth behavior, life prediction, modeling,
14	02		automated test control, material characterization,
11/20	06/11		

19. ABSTRACT (Continue on reverse if necessary and identify by block number)

The design of high performance aircraft engines requires the development of reliable life-prediction methodology to aid in the evaluation and safety of the critical engine components. A comprehensive multi-task research and development program was conducted to establish a sound life-prediction methodology. The program consisted mainly of (1) Experimental investigations and analytical modeling of crack growth behavior, (2) Experimental investigation of mechanical properties and performance characteristics of structural materials, (3) Environmental effect on elevated temperature mechanical behavior, and (4) Development of test techniques, upgrading, and maintenance of the AFWAL/MLLN Mechanical Test Facility.

The progress in the program is summarized according to the following major tasks -- experimental developments, crack growth characteristics,

20. DISTRIBUTION/AVAILABILITY OF ABSTRACT UNCLASSIFIED/UNLIMITED ☐ SAME AS RPT. ☒ DTIC USERS ☐	21. ABSTRACT SECURITY CLASSIFICATION Unclassified	
22a. NAME OF RESPONSIBLE INDIVIDUAL T. Nicholas	22b. TELEPHONE NUMBER (Include Area Code) (513) 255-2689	22c. OFFICE SYMBOL AFWAL/MLLN

DD FORM 1473, 83 APR   EDITION OF 1 JAN 73 IS OBSOLETE.

Block 19 (Continued)

analytical investigations, and evaluation of mechanical properties. In the area of experimental developments, computer control systems and associated software were developed to automate most of the manually operated servo-hydraulic test systems. A data processing and archival system with appropriate software was developed. Compliance investigations were conducted and the electric potential technique was utilized for crack length measurement. A thermal-mechanical fatigue test rig was set up and HCF/LCF capability was enhanced. A vacuum system for elevated temperature fatigue crack growth tests was designed and fabricated. A laser interferometry system for the evaluation of interior crack surface opening was developed. An IDG rotating mirror system was interfaced with a PDP 11/24 for short crack investigation and an actuator system for the Theta Ring was designed.
    Extensive research was conducted in the areas of creep/fatigue interaction, HCF/LCF behavior, creep crack growth in laboratory air, environmental effects on mechanical properties, threshold behavior, and modeling of crack growth behavior to determine the basis for sound life-prediction methodology.
    To aid the development of life-prediction methodology, various analytical investigations were conducted which included the development of a constitutive model for a porous process zone, the evaluation of uniaxial cyclical stress-strain behavior using Bodner-Partom constitutive model, the effects of mesh-analysis of SEN specimens, the enhancements to finite element program, the effects of size and geometry on nonlinear correlation parameters, the use of alternating method to analyze curved crack front in ring specimens, and the application of the SNAP program.
    Various types of mechanical tests such as uniaxial tension, compression, creep fatigue, low cycle fatigue, and fatigue crack growth rate were conducted on a variety of structural materials including nickel-base superalloys and alloys of titanium and aluminum.

Block 18 (Continued)

mechanical properties, environment effects, elevated temperature tests, nickel-base superalloy, gas turbine engine and aircraft structural materials, laser interferometry, electric potential, compliance determination and application.

FOREWORD

The work described in this report was supported by the Metals Behavior Branch, Metals and Ceramics Division, Materials Laboratory, Air Force Wright Aeronautical Laboratories (AFWAL/MLLN) under Contract F33615-81-C-5015, "Research on Mechanical Properties for Life Prediction," with the University of Dayton Research Institute (UDRI). The contract was administered under the direction of AFWAL by Dr. Theodore Nicholas, MLLN. The program was performed at the Mechanical Test Facility of AFWAL/MLLN with Dr. Noel Ashbaugh as the Principal Investigator reporting to the UDRI Structural Integrity Division Manager, Dr. Joseph P. Gallagher.

Scientific/engineering investigations were conducted by Drs. M. Khobaib and T. Weerasooriya and Mr. George Hartman. Analytical investigations and finite element analyses were supported by Dr. A. M. Rajendran. The HCF/LCF crack growth effort was under the direction of Dr. A. M. Brown and the test system development for high frequency load application was supported by Messrs. Richard Goodman and D. J. Koester. Fabrication of test systems and the generation of crack growth data and other mechanical property information was accomplished by Mr. D. C. Maxwell, Mr. G. R. Ahrens, Mrs. S. W. Ramsey, Mr. D. A. Johnson, and Mr. W. R. Goddard. Additional technician support was provided by Messrs. R. W. Tait, G. E. Terborg, and R. A. Albrecht. This manuscript was typed with diligence by Miss Debbie Garner.

iii

The work was conducted during the period 15 June 1981 to 30 September 1984.

TABLE OF CONTENTS

v

TABLE OF CONTENTS (Continued)

TABLE OF CONTENTS (Continued)

TABLE OF CONTENTS (Continued)

TABLE OF CONTENTS (Concluded)

LIST OF ILLUSTRATIONS

LIST OF ILLUSTRATIONS (Concluded)

LIST OF TABLES

SECTION 1

INTRODUCTION

Traditional design procedures for gas-turbine-engine components are responsible for an adverse economic impact upon the projected costs to the Air Force for maintenance and replacement of these components, especially in view of the higher performance requirements being imposed on future aircraft engines. Improved performance is gained by increasing the engine rpm which produces higher stress in the components and by raising the nominal engine operating temperature which promotes environmental attack and enhances degradation of the material. The combination of higher operating stresses, temperature, and aggressive environmental conditions has fostered the strong emphasis by the Air Force on the development of life-prediction methodology to aid in the evaluation of the safety of the critical engine components.

To develop a sound life-prediction methodology, the University of Dayton Research Institute (UDRI) has undertaken a comprehensive multi-task research and exploratory development program comprising (1) experimental investigations and analytical models of fundamental crack-growth (CG) behavior in engine materials under engine operating conditions, (2) theoretical investigations to determine and evaluate criteria governing CG, (3) experimental investigations to determine the mechanical properties and performance characteristics of

1

existing and candidate engine and airframe materials, (4) environmental effect on elevated temperature mechanical behavior, (5) development of test techniques and instrumentation applicable to life-prediction technology, (6) maintenance, scheduling, and operation of equipment required to perform this program, and (7) dissemination and procurement of scientific information.

The progress in this program, which is described in more detail in the following sections of this report is outlined below:

Experimental Developments -

- Automation of Test Systems
- Data Processing System and Software
- Compliance Investigations
- Electric Potential Application
- Thermal-Mechanical Fatigue Crack Growth
- HCF/LCF Capability
- Vacuum System for Fatigue Crack Growth Tests
- Development of a Laser Interferometry System for Interior Crack Surface Opening
- Actuator System for Theta Ring
- Interfacing PDP 11/24 and IDG Rotating Mirror System
- Nonlinear Structural Response and Friction Damping

2

Crack Growth Characteristics -

- Creep/Fatigue Interaction

- HCF/LCF Behavior

- Creep Crack Growth in Laboratory Air

- Environmental Effects

- Threshold Behavior

- Modeling Crack Growth Behavior

Analytical Investigations -

- Constitutive Model for Porous Process Zone

- Uniaxial Cyclic Stress-Strain Behavior Using
  Bodner-Partom Model

- Effects of Mesh-Analysis of SEN Specimen

- Finite Element Program Enhancements

- Effects of Size and Geometry on Nonlinear
  Correlation Parameters

- Use of Alternating Method to Analyze Curved
  Crack Front in Ring Specimen

- SNAP Program

Evaluation of Mechanical Properties

- Description, Types of Tests, and Materials

- Reports and Documentation of Data

3

SECTION 2

EXPERIMENTAL DEVELOPMENTS

A portion of this program involved the development and assembly of equipment and instrumentation to conduct, control, and evaluate a variety of advanced mechanical tests. The automation of test systems was of primary importance for the following reasons:

- Control of test is based on calculated parameters.
- Crack lengths are determined automatically.
- Control of test is based on crack length.
- Data are acquired automatically.
- Data are generated consistently and efficiently.
- Test machines are operated 24 hours a day.
- Personnel are used more effectively.

Some new experimental capabilities were developed and utilized for the following investigations:

- The determination of crack lengths from compliance and electric potential measurements,
- The study of crack growth behavior under thermal-mechanical fatigue conditions and combined high cycle and low cycle fatigue (HCF/LCF) loads,
- The evaluation of crack growth behavior in vacuum,

4

- The measurement of interior crack opening in a transparent material,

- The computer control of an interferometric displacement gage using rotating mirrors,

- The evaluation of nonlinear structural response and friction damping, and

- The excitation of a high frequency resonance loading ring.

Additional hardware and programs for data analysis have been designed and developed to support the archival, retrieval, and reduction of the experimental data on a central computer system.

A discussion of these experimental developments is presented in the following sections.

2.1 AUTOMATION OF TEST SYSTEMS

Several types of control systems employing micro- and mini-computers have been developed for various material test systems in the laboratory. The choice of computers in these systems was influenced by the following factors:

- The control requirements,

- The previously developed hardware and software,

- The ease of procurement of the computer,

- The current computer technology, and

- The current state-of-the-art hardware and software support for a computer.

Since the impact of these factors varied throughout the performance of the program, many makes of computers -- VIC-20, TEK 4051 and 4052, IBM PC, PDP 11/24, and IBM CS9000 -- were utilized in the control systems.

Software programs for these systems were developed to provide specific types of control for the research investigations, to monitor and acquire data, and to facilitate modifications of the software so that the requirements in future investigations can be implemented. To expedite the development of software, a portion of these programs included software that the Structural Integrity Division of the UDRI had previously developed.

The types of test control and test monitoring that the systems provide are listed in Table 1. A summary of the computers and the applications of the control systems is shown in Table 2.

2.1.1   Crack Growth Tests

TABLE 1

APPLICATIONS OF COMPUTER SYSTEMS

FCG: Fatigue Crack Growth Under the Conditions –
              Constant Load Range
              Constant Stress Intensity Range
              Threshold with Exponential Decay
              Precracking Specimens

HTCG: Combined Hold-Times and Fatigue Cycles

TMFCG: Thermal Mechanical Fatigue Crack Growth

HCF/LCF: High Cycle and Low Cycle Fatigue

PUR: Partial Unloading and Reloading of a Crack
            Growth Specimen

LC: Load Control

DP: Data Processing

ADN: Acquisition of Data and Monitoring (Any of the
            Following) –
              Displacement
              Load
              Compliance
              Temperature
              Cycle Count
              Current Time

HT: Temperature Spectrum for Heat Treatment

TABLE 2

COMPUTER CONTROL SYSTEMS

System Computer	Type[1] of Test Frame	Application[2]	Specimen Geometry[3]	Crack Length Determination[4]
IBM PC	S-H	FCG, HTCG	C(T), M(T), SE(T), EC(T)	CMOD Compliance BFS Compliance
IBM CS9000	S-H	FCG TMFCG	C(T), M(T), SE(T), EC(T) M(T)	CMOD Compliance Electric Potential
PDP 11/24	S-H ES with S-H	FCG HCF/LCF DP	C(T), SE(T), EC(T) M(T) All	CMOD Compliance Electric Potential ___
TEK 4052	S-H	FCG, HTCG	C(T)	CMOD Compliance Electric Potential
TEK 4051	CF	ADM, PUR	C(T), M(T)	LLD Compliance
VIC-20	ES with PC Resonance	HCF/LCF LC HT	Axial Fatigue Axial Fatigue Material Samples	— — —

(1) S-H: Servo-Hydraulic; ES: Electro-Magnetic Shaker; CF: Creep Frame; PC: Pneumatic Chamber

(2) See Table 1 for Definition of Notation

(3) Crack Growth Specimen Notation Given in ASTM E616 Except EC(T) is a Compact Specimen with H/W = 0.483

(4) CMOD: Crack Mouth Opening Displacement; BFS: Back-Face Strain; LLD: Load-Line Displacement

2.1.1.1   IBM 9000 System

Software was developed for the IBM System 9000 microcomputer to perform four types of laboratory crack growth tests. These are constant load amplitude, constant stress intensity amplitude, decreasing stress intensity precracking (ASTM E399), and decreasing stress intensity threshold. These four types of tests can be performed on a variety of specimen geometries including the compact type, C(T) and the center crack type, M(T).

The program uses crack mouth opening displacement compliance to determine crack length. The test control, operator interface, and data display are real-time interactive functions and the test data acquisition and control are completely automated. The software written in FORTRAN is currently installed on three computers in the laboratory.

2.1.1.2   IBM PC System

The application of the IBM PC based system was very similar to that described for the IBM 9000 (Section 2.1.1.1). The major portion of the software was developed using BASIC language. Thus the software can be modified to support other interests and to meet changes in test requirements. Two subroutines in the software were developed in machine language under UDRI support to facilitate the printing of graphs displayed on the CRT and to provide rapid data

acquisition. To provide near real-time control, the BASIC language program was compiled using the IBM Basic Compiler software.

The software was modified so that tests can be performed under hold-time conditions and simple spectrum type load. Also, an investigation was initiated to support the incorporation of back-face strain measurements into the control software.

2.1.1.3 Tektronix 4052 System

A computer control system was developed to study the interaction of frequency, temperature, stress ratio, maximum stress intensity factor, and hold-time on crack growth rate behavior. A description of the test system hardware is given in Appendix A. The software was written in BASIC language.

Crack length is monitored by either compliance or electric potential method. Real-time crack length is used to control the load on the specimen to attain a specified history of stress intensity.

The control system has generated data on the effects of frequency, temperature, stress intensity ratio, maximum stress intensity, hold-time, and complex waveshapes on crack growth behavior.

10

2.1.1.4   PDP 11/24 System for FCG

The application of the PDP 11/24 based
system was similar to the IBM 9000 and PC systems. It provided
the capability of precracking, constant K range, constant load
range, and threshold tests for three different specimen
geometries. Operator interruptable menu capability was
installed to facilitate the use of the system. A description
of the system hardware and subroutines is given in Appendix B.
In this system, CMOD compliance was used to determine crack
length.

2.1.1.5   PDP 11/24 HCF/LCF System

A control system using a PDP 11/24 was
assembled to conduct HCF/LCF tests on the Instron Major/Minor
machine. The crack length was determined using an AC electric
potential system which was interfaced to the computer.

An HCF/LCF test requires the control of
two load amplitudes -- a high cycle load and a low cycle load.
The system was designed to consider preselected loading
functions in both load amplitudes. Usually, the tests had been
conducted under a linearly decreasing stress intensity range
for the high cycle load as a function of crack length and a
constant stress intensity range for the low cycle load. The
software for the system was developed using FORTRAN. Also, to

expedite the testing, the software included a precracking routine.

2.1.2 Creep Laboratory Data Acquisition - TEK 4051

A data acquisition and control system using a Tektronix 4051 microcomputer was developed to monitor and control up to nine creep tests simultaneously. The Tektronix computer was interfaced to a Daytronics signal conditioning unit which contained all the necessary electronics to provide high level analog outputs from LVDT's, strain gages, thermocouples, and other transducers.

The Tektronix computer can interrogate the Daytronic signal conditioning unit via the IEEE-488 bus to acquire data and time/date information. The operator can specify which Daytronic channels are to be sampled (those to which test instruments were connected) and the sampling rate to match the test requirements.

The system has the capability to trigger the unloading and reloading of individual test frames. In standard creep rupture testing, this capability is used to load the specimen initially and to unload it when the test is completed. For creep crack growth testing, the loading/unloading capability can be used periodically to partially unload and load the specimen to generate a load-displacement plot.

Specimen compliance is calculated from a load-displacement plot and stored. The crack length can be calculated during the data processing phase using the compliance calibration for many common geometries. With the ability to compute compliance, the Tektronix monitors automated creep crack growth tests with a minimum of operator supervision.

The system provides interactive test control and data display functions so that the operator can monitor the test as required. All data is stored on an integral magnetic tape drive and software is available to transfer this data over the RS-232 serial port to other computers within the laboratory.

2.1.3   VIC-20 Applications

Many laboratory tests and experimental procedures require the continuous data acquisition and control of one or more variables to maintain proper test conditions. It is often impractical to perform these functions manually 24 hours a day. Micro- and mini-computers have been purchased to automate much of the testing equipment in the laboratory. However, there are several cases where the cost of existing micro- and mini-computer systems is not justified for the intended application.

The first application of a VIC-20 system was to provide an inexpensive control system for the Schenck resonant machines. As the capabilities of the unit became apparent, additional applications were identified and the necessary interface hardware was designed and built. At the present time, three applications have been identified:

1. Control of Schenck resonant fatigue testing machines,

2. Control of a furnace used for automated heat treating, and

3. Control of data acquisition for an electropneumatic shaker system used for crack growth studies.

2.1.3.1 Schenck Fatigue Machines

Several Schenck fatigue machines have been used in the laboratory to conduct fatigue tests. All of the control systems for these machines were over 30 years old and were in poor condition. A prototype analog control system was built and proved to be functional. However, this system was expensive to construct and install and was difficult for new operators to learn.

The VIC-20 control system was developed as an alternative. The system which maintained the desired

load and provided the cycle count was inexpensive to construct
and to install and has been easy to operate.

2.1.3.2   Furnace Controller

The automated furnace controller was
designed to eliminate the need for manual 24 hour monitoring of
heat treatments. Many of these heat treatments require a
constant heating or cooling rate. The existing manual controls
required constant setpoint adjustments by the operator. The
VIC-20 system allowed the operator to set up the desired heat
treatment temperature profile and the computer would complete
the heat treatment cycle.

2.1.3.3   HCF/LCF Test Systems

The control and data acquisition systems
for the C10 and C20 electropneumatic shaker units used for HCF/LCF
tests were developed. The simplest computer configuration on the
C10 system performs the following functions:

1. Cycles the major load at the desired intervals.

2. Monitors the elapsed time of the test.

3. Monitors the number of major cycles completed.

4. Halts the test after a prespecified number of
    major cycles.

5. Provides fail safe shut-down of the power
    amplifier and specimen heaters.

The VIC-20 for the C20 HCF/LCF system
provides the following functions:

1. Full servo-control of major and minor loads.

2. The monitoring of major cycle count, major and
   minor loads, elapsed test time, and electric
   potential.

3. Load shedding for crack growth testing. The
   parameters for the load shedding may be
   changed during the test by menu selection.

4. Hard copy data at preselected interval of major
   cycles.

5. Interruption of the test at preselected major
   cycle count.

6. Fail-safe shut-down.

7. Standard trapezoidal load waveform or a programmed
   profile (20 steps). Dwell time at each step is
   selectable and major and minor loads may be
   independently specified at each step.

2.2   DATA PROCESSING SYSTEM

The data processing system was developed as part of the
automation of test systems. The system hardware and the
software developed for data analysis, reduction, plotting,

etc., for tests conducted in the laboratory are described in the following paragraphs.

2.2.1   System Hardware - PDP 11/24

To efficiently utilize the microcomputers assigned to each test station, it was necessary to provide a means of transferring test data from the local microcomputers to a central processor capable of supporting the data reduction, plotting, and report generating needs of the scientific and engineering personnel. A Digital Equipment Corporation (DEC) PDP 11/24 computer with 18 RS-232 serial lines was installed as a central processor (HOST) to provide the required computing environment. Some of the serial lines are dedicated to terminals in a user's computing area. The rest of the lines are connected to the microcomputers at the test stations.

The 11/24 processor supports two graphics terminals and an HP digital plotter. The graphics terminals provide rapid data evaluation and interactive plotting capabilities. The digital plotter provides interactive hardcopy capability and can produce high resolution report quality graphics and is currently being used for these purposes.

17

The 11/24 system is equipped with 10 megabyte removable cartridge disk drives. These units allow data to be permanently archived on removable cartridges as required. In addition, all data are backed-up on cartridge tapes using a streaming tape drive unit connected to the system.

2.2.2   Software on the PDP 11/24

Laboratory data reduction and display software were developed on the HOST computer. This software was designed to provide the specific data reduction tools required as well as general purpose data display and manipulation routines. Table 3 contains a list of software routines currently available on the HOST 11/24 computer.

Data reduction software includes a general fatigue/creep crack growth reduction package which produces crack growth rate and stress intensity data for a wide variety of specimen geometries and input data formats, a data manipulation routine which operates on columnar data files, and several other routines. Data display software includes an interactive plotting package which drives the digital plotter and a parallel package which drives the graphics terminals.

All software is designed to accept a standard header format which contains sufficient information to identify the data in the file. Most of the routines are written to encourage the operator to enter as much relevant information as

18

TABLE 3

PROGRAMS MAINTAINED ON HOST COMPUTER

NAME	FUNCTION
CHANGE	Modifies Entire Columns of Data Files
CRPRED	Converts Data from Creep Area into Usable Format
DADNDT	Standard Reduction Program for Fatigue and Creep
DIGIT	Digitizes Data Plots
DINPUT	Input Program for Keying in DADNDT Data
HCFLCF	Reduction Program for High Cycle/Low Cycle Fatigue Data
LASER	Reduction Program for LASER Interferometry Data
PLOT	Plots Data on Hewlett-Packard 7221C Plotter
POLYFT	Calculates nth-degree Polynomial Curve Fit of Data
RPPLOT	Creates Report Quality Plots on Hewlett-Packard 7221C Plotter
SPLINE	Reduction Program for LASER Interferometry Data
SPLOT	Version of PLOT to Drive TEK 4014 Graphics Terminal
SRTCRP	Sorts Data from Creep Laboratory
TEXT	Text Writing Program for Hewlett-Packard 7221C Plotter

possible. Full data documentation is thus a part of the data processing procedure from the initial stages.

2.3   COMPLIANCE MEASUREMENTS AND TECHNIQUES

In a linear elastic analysis of typical crack specimens, the slope of the load versus crack mouth opening displacement (CMOD) is a single valued function of the crack length. In addition, displacements and/or strains can be determined at other locations to obtain other functions of crack length. The functional relationship between the inverse of the slope, known as the compliance C, and the crack length can be either experimentally evaluated or analytically computed via finite element method for a given cracked geometry. Once the functional relationship between compliance and crack length is known, crack length can be determined after the compliance is evaluated by experimental methods. Techniques have been applied and developed, when necessary, to determine crack length by compliance methods for the following situations.

2.3.1   Compliance Application in Automated Crack Growth Tests

In the development of automated testing, crack length measurement via compliance is the major input. Digitized load and CMOD data are acquired by various types of computers as a function of time. Depending on the computer

set-up, 250 to 1500 sample data points are acquired by the computer. The computer is used to numerically evaluate the compliance on real-time by fitting a least square linear regression line to load-CMOD data within a user-defined load window. The user has the option to determine the compliance window to isolate the linear portion in the total load range after graphical observation of the load CMOD trace.

The system that has been developed incorporates the relationships for crack length as a function of compliance for widely used specimen geometries. Once the value of compliance is determined, crack length (a_{comp}) is obtained from the functional relationship

$$a_{comp} = Wf_1 \ (EBC),\qquad(1)$$

where B is thickness, E is an effective modulus, W is a characteristic dimension, and f_1 is a nondimensional function.

It has been observed that the crack length estimates for a test can be improved if the operator obtains an effective modulus value at the start of the test for a known crack length from

$$E = 1/(BC) \ f_2 \ (a_{given}/W),\qquad(2)$$

where f_2 is a nondimensional function. Based on experience,

once an effective modulus value has been determined, the test can proceed without further operator intervention to change E.

For the case where new constant temperature levels are selected within a test, new effective modulus values need to be determined from Equation 2 at each temperature level. On the reasonable assumption that the length of the crack is the same before and after the temperature change,

$$E_{new}/E_{old} = C_{old}/C_{new}. \qquad (3)$$

Once the new compliance is measured after the temperature change, E_{new} could be computed using Equation 3.

In tests where cracks were grown at different isothermal segments of temperatures, the difference between crack lengths both computed from compliance and measured optically at the end of the experiment was less than .020 in. for cracks over an inch long. Conditions in some tests included variations in frequency, temperature, hold-time, and waveform with total test times as long as four months.

For a stationary crack at high temperature, repeated measurements using a compliance technique yielded a standard deviation of 0.0015 in. for the crack length value. Long term stability of crack lengths determined by compliance has been found to be far superior to the crack lengths

determined by electric potential. However, the resolution of changes in crack lengths determined by compliance techniques has been an order of magnitude lower than changes determined by electric potential. Thus, crack length measurement by compliance is superior in automated applications for high temperature long term tests such as sustained load, threshold, and tests in oxidizing environments.

One of the major problems of the compliance method using an axial extensometer is that this method is limited to low loading frequencies, e.g., below 3 Hz. This problem results both from the inability to secure the high temperature extensometer properly to the specimens and from the resonances of the extensometer assembly at higher frequencies.

2.3.2   CMOD Application at Room Temperature

At room temperature, a CMOD clip gage similar to that recommended by ASTM Standard Test Method E399 is used. This type of gage is used for precracking and crack growth tests in laboratory specimens.

Fatigue crack growth rate studies were conducted on 16 C(T) specimens of X7091 aluminum. Crack growth rates were determined by visual crack length measurements and CMOD compliance measurement. The curves of crack growth rate versus stress intensity factor from COD compliance measurements

were compared to the optical crack growth rate results which were determined by following ASTM E647 Standard Test Method for Constant-Load-Amplitude Fatigue Crack Growth Rates Above 10^{-8} m/cycle. Differences between the growth rates from the two methods are discussed in terms of potential errors in the evaluation of variables used in the data collection and analysis. This effort was discussed in detail in Reference 1.

2.3.3   Back-Face Strain

Nonvisual crack length determination for use in crack growth behavior studies can be accomplished with strain measurements on a compact type specimen. This method of crack length determination is well suited for use with closed-loop computer controlled test systems.

A finite element analysis provided the theoretical back-face strain values for crack-length-to-width ratios from 0.2 to 0.8. Then, a mathematical relationship was determined for the crack length ratio as a function of back-face strain compliance. The crack lengths calculated from strain compliance were compared to those calculated from CMOD compliance. The crack length ratios computed from the measured strain compliance varied by approximately +2 percent at a/W = 0.2 to -2 percent at a/W = 0.8 from the ratios computed from the CMOD compliance. A second strain measurement location which enhanced the sensitivity of the back-face strain

24

compliance for crack length ratios from 0.2 to 0.5 was determined from the results of the finite element analysis. A mathematical relationship for the crack length ratio as a function of the dual-location strain compliance was also derived. The crack length ratios calculated from both dual-location strain compliance and CMOD compliance were compared and the ratios were within one percent over the range of a/W values from 0.2 to 0.8. More details can be found in Reference 2.

2.3.4 Compliance Determination During Creep Tests

Since equipment was readily available in the laboratory to measure specimen displacement under sustained load at elevated temperatures, techniques were evaluated to determine if the specimen displacement measurements could be used to determine crack lengths. The results of these evaluations have been described in References 3 and 4.

In summary, it was determined that the values of the displacement divided by the applied load could not be correlated with the crack length in a specimen. However, the compliance from the linear portion of the load-displacement data obtained from a partial unloading of the specimen could generally be correlated with crack length. Some anomolous behavior in the compliance determination at the start of a sustained load test has been discussed in Reference 3.

The compliance methodology also provided a reasonable characterization of crack lengths in specimens with extremely curved or tunneled cracks, References 4 and 5. The technique was also especially useful for specimens with side-grooves which made the optical viewing of the crack tips difficult.

2.3.5   Compliance Determination in the Inelastic Range

Compliance measurements were made during creep and fatigue crack growth to establish crack length. During various tests, data from several nickel-base superalloys demonstrated a lack of a one-to-one correspondence between crack lengths and compliance values. In particular, decreases in compliance were observed when going from fatigue to creep and when going from low frequency to higher frequency fatigue cycling. On the other hand, no anomalous behavior was observed in the compliance measurements of ductile copper which was loaded to successively higher K values. It is concluded that a probable cause of the anomalous compliance values during transient loading conditions is due to a complex three-dimensional stress state which may be additionally influenced by environmental factors. Details of the conditions for the compliance measurements and of the anomalous behavior are discussed in Reference 3.

2.3.6 High Temperature Crack Length Determination

For high temperature crack length measurement, a modified MTS high temperature axial extensometer is used in the laboratory. The extensometer is connected to the specimen through a pair of quartz rods. The total extensometer assembly along with the quartz rods is attached to the specimen by spring loading the assembly into two tiny impressions located across the crack mouth of the specimen. Extensometers are either water or air cooled. With this set-up, crack lengths ' have been determined at test frequencies up to 5 Hz and test temperatures up to 1800F.

2.3.7 Interferometric Displacement Gage (IDG) Applications

2.3.7.1 IDG Description

The measurement of specimen displacements can be accomplished by using a unique laser IDG originally developed by Sharpe et al. [6]. The method utilizes the coherent light of the Ne-He laser to make precise measurements of displacement by monitoring the movement of interference fringes that are formed by laser light impinging on two pyramidal indents that are across the crack, as shown in Figure 1.
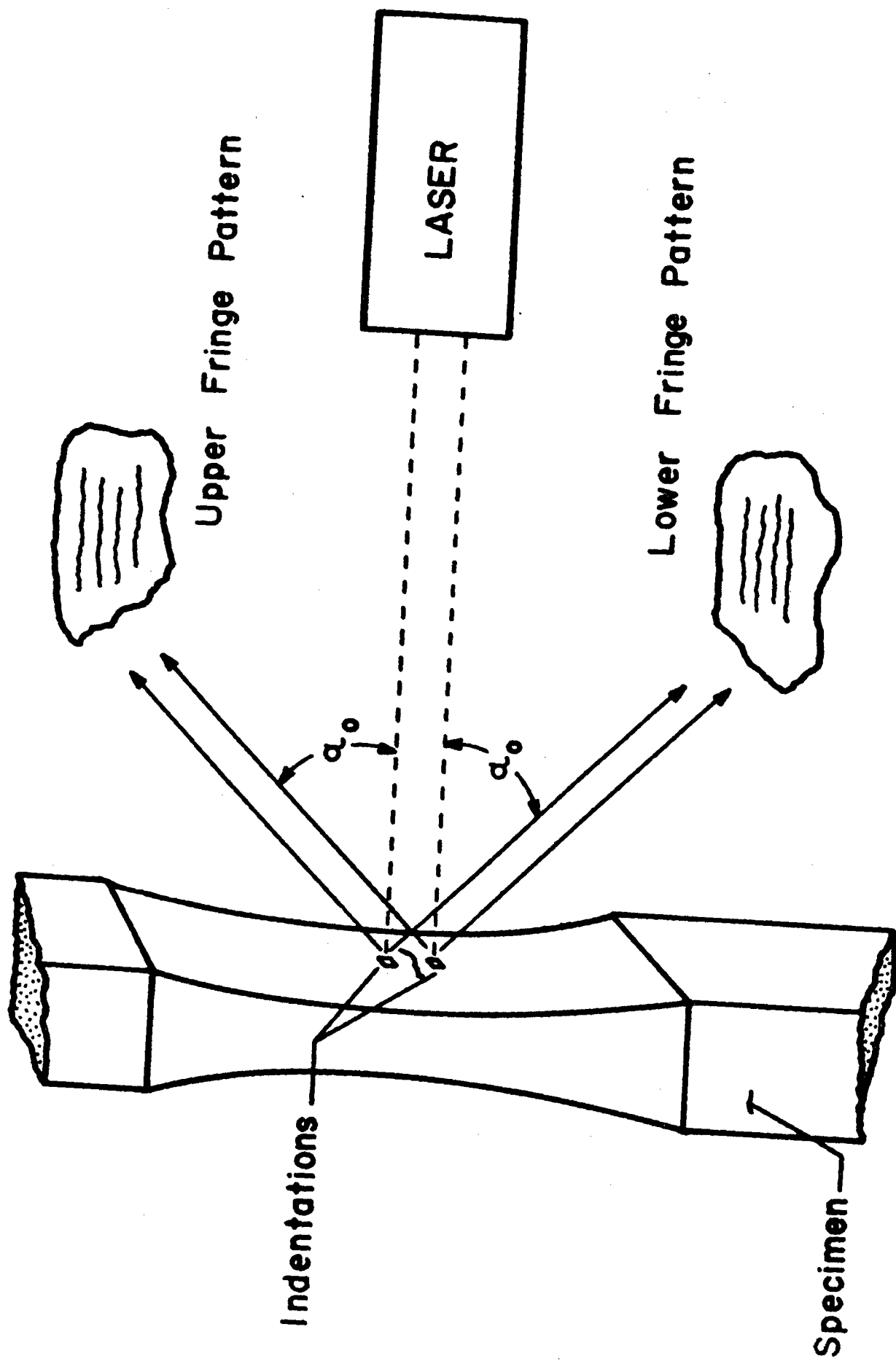
Figure 1.   Schematic Illustration of the Principle of Operation of the Interferometric Displacement Gage.

Movement of the indents are related to the movement of fringes that are formed in space. Counting of the fringes that pass by fixed observation points provides the information to determine the relative displacement of the indents that straddle the crack. The system that is based on fixed observation points is called the fixed mirror system in subsequent discussion.

Resolution of the system can be increased a 100 fold by monitoring the fractional movement of the fringes in space. The system employs servo-controlled rotating mirrors to sweep the fringe patterns across the stationary detectors. The rotating mirrors allow the system to monitor fractional fringes as a function of time (or load applied to the specimen). A schematic of the automated system is shown in Figure 2.

The system was automated using a PDP 11/24 mini-computer and was able to produce real-time load-displacement curves with resolution of 100 A.

2.3.7.2   IDG Application at Room Temperature

The fixed and rotating IDG systems have been used in the laboratory to measure the displacement between two indents approximately 15 µm across and with a
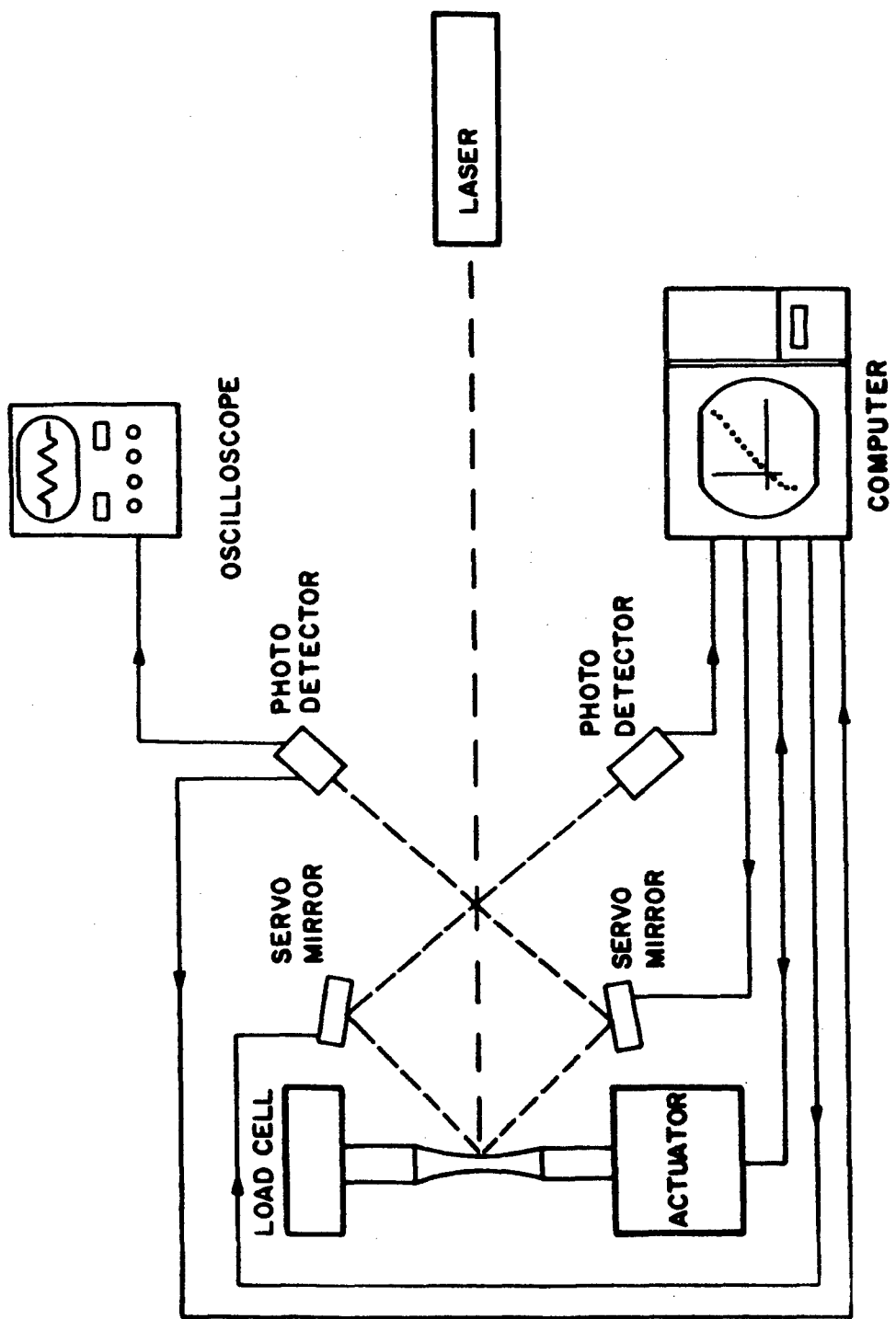
Figure 2. Schematic Illustration of the Computerized Interferometric System.

separation as small as 40 μm. The rotating mirror system is capable of measuring displacements as small as 100 A while the fixed mirror system measures displacements on the order of 0.5 μm.

As a result of the size of the indents and the ability to measure very small displacements, the rotating mirror IDG has been applied to the study of the growth of naturally initiated cracks. In addition, estimates of crack lengths greater than 50 μm can be obtained from the compliance of the load versus CMOD for surface flaws. The closure load of the small crack (see Section 2.3.8) and the extent of crack closure during the unloading process can also be determined.

2.3.7.3 A Laser IDG System Application at High Temperature

The fixed mirror IDG system incorporating a Tektronix 4051 microcomputer for data acquisition has been used in the study of long crack growth behavior under conditions of both sustained and fatigue loading. For high temperature applications up to 1200F, furnaces were modified to accomodate laser illumination and reflection from the indents across the long crack in a C(T) specimen. Crack lengths were determined from the compliance of the load displacement trace. Displacement was evaluated by counting the number of total fringes passing a fixed point in space.

2.3.8 Closure Evaluation

Information in the literature indicates that the
phenomenon of crack closure affects the fatigue crack growth
behavior, and hence, the life of components under fatigue
loads. Crack closure, itself, is affected by the prior loading
history. However, there is lack of information on the
consistency of measured values of crack closure. The behavior
of crack opening and closing was evaluated and measured by
three methods -- clip gage, back-face strain, and IDG. The first
two methods provide far-field measurements and the last method,
IDG, provides near tip behavior. The results from these three
methods, when applied to several loading histories, have been
presented in Reference 7.

2.4 ELECTRIC POTENTIAL APPLICATION

The potential drop crack measurement system is a method
of estimating crack length in a specimen by measuring the
voltage across the crack when a current is passed through the
specimen. A constant current amplitude is maintained through
the specimen and the voltage across the crack is measured as
the crack grows. Functional relationships between crack length
and voltage across the crack must be determined either
analytically or from empirical data for a specimen
configuration and location of the voltage probes. Once a
relationship is obtained, the crack length can be computed from
the voltage readings.

Typical relationship between the measured electric
potential (V) and the crack length (a) has the form

$$V/V_0 = g_2 \ (a/W), \qquad\qquad (4)$$

and for the inverse

$$a_{elec} = Wg_1 \ (V/V_0), \qquad\qquad (5)$$

where W is a characteristic specimen dimension, V_0 is the
reference voltage for a known crack length, e.g., notch length,
and g_1 and g_2 are nondimensional calibration functions.

An important assumption in the application of the method
is that the voltage across the crack is a function of crack
length only. Many other factors which can affect the voltage
depend on the test conditions and whether a DC or AC system is
used.

2.4.1   DC Potential System

At room temperature in a nonoxidizing
environment, voltage is typically a function of crack length.
However, most of the material tests are performed in laboratory
air at elevated temperatures, i.e., oxidizing environment.
Under these conditions, the voltage is influenced by several
factors which must be taken into account in order to produce

accurate crack length information using the DC potential technique.

Four factors which most commonly account for errors in the data are: (1) resistivity changes in the material as a function of temperature, (2) thermal EMF generated by temperature differences at the voltage measurement points, (3) voltage drops caused by oxide bridging across the crack surfaces, and (4) long term effects. Most of the DC potential development effort has been directed toward isolating and correcting these factors.

2.4.1.1 Resistivity Effect

Material resistivity changes with temperature are most easily minimized by maintaining accurate temperature control during the test. The typical temperature controllers and furnace equipment in the laboratory are capable of providing acceptable control by properly insulating furnace openings and adjusting control settings. In cases where nonisothermal tests are being conducted (thermal mechanical fatigue), electric potential readings must all be taken at the same temperature to minimize the effects of material resistivity changes. This limits the data acquisition rate to a maximum of two readings per thermal cycle. Normally, this is not a problem for typical crack growth rates on nickel-base superalloys.

2.4.1.2   Thermal EMF Effect

Thermal EMF is a voltage which is generated due to thermocouple effects at the junction of the voltage measurement wires and the specimen. The effect is only produced when the temperature at the two voltage measurement junctions is not the same or when different materials are used as measurement wires. Methods that reduce the effect of the thermal EMF include maintaining accurate temperature control which would minimize material resistivity effects and selecting voltage measurement wire materials which have an inherently low thermal EMF when used with the material being tested. For use with IN718, we have found that Nichrome wires produce a very low thermal EMF as compared with conventional thermocouple materials such as Chromel or Alumel. Nichrome may also be useful with other nickel-base superalloys.

In addition to minimizing the thermal EMF using the techniques described above, it is possible to correct the remaining error by making a voltage reading after turning off the current through the specimen. The voltage measurement made in this way reflects only the thermal EMF and can be subtracted from a subsequent reading to produce a voltage which does not include thermal EMF effects. With the advent of digital programmable power supplies and voltmeters, this technique lends itself to automation with microcomputers

and most of the electric potential work within the laboratory
is now performed in an automated fashion.

2.4.1.3   Oxide Bridging Effect

Another source of error in the DC
potential technique has been oxide bridging of the crack
surfaces primarily during slow crack growth or static creep
crack growth testing at intermediate temperatures. This
phenomenon has not proved to be as significant as initially
thought and no effective techniques have been developed to
eliminate this problem yet.

2.4.1.4   Long Term Effects

In long term crack growth experiments,
the stability of electric potential system has become a
concern. The lack of stability is probably due to the
deterioration of the junction of the potential leads, the
specimen and to the combined effects of the three previously
discussed factors. In these situations, electric potential
crack measuring technique is used as an interpolating device
only.

For tests where long term effects
influence the potential values, V_0 is updated from Equation 4
for a known crack length which is either measured optically or

obtained from a compliance measurement. Then, for the short term the new V_0 is used in Equation 5 for the evaluation of crack length.

2.4.2   AC Electric Potential on HCF/LCF Tests

An AC electric potential measurement system was used in one of the automated HCF/LCF testing systems for crack length determination. The potential system was patterned after the one used in Reference 8. A block diagram of the system is shown in Figure 3.

Most of the factors which affected the determination of crack length in a DC potential system (see previous section) influence the readings of the AC system. However, the EMF effect was eliminated with the application of the AC system. Additional factors which included an inducted capacitence attributable or due to the presence of the crack influenced the potential measurements. A major advantage in the application of an AC potential system was that the lock-in amplifier monitored only the desired signal, while rejecting noise.

The AC system was used to evaluate fatigue crack growth behavior in M(T) specimens of Inconel 718 under a combined major/minor cycle loading at temperatures up to 649C (1200F). The specimens were tested under conditions of

37

AC POTENTIAL SYSTEM SCHEMATIC
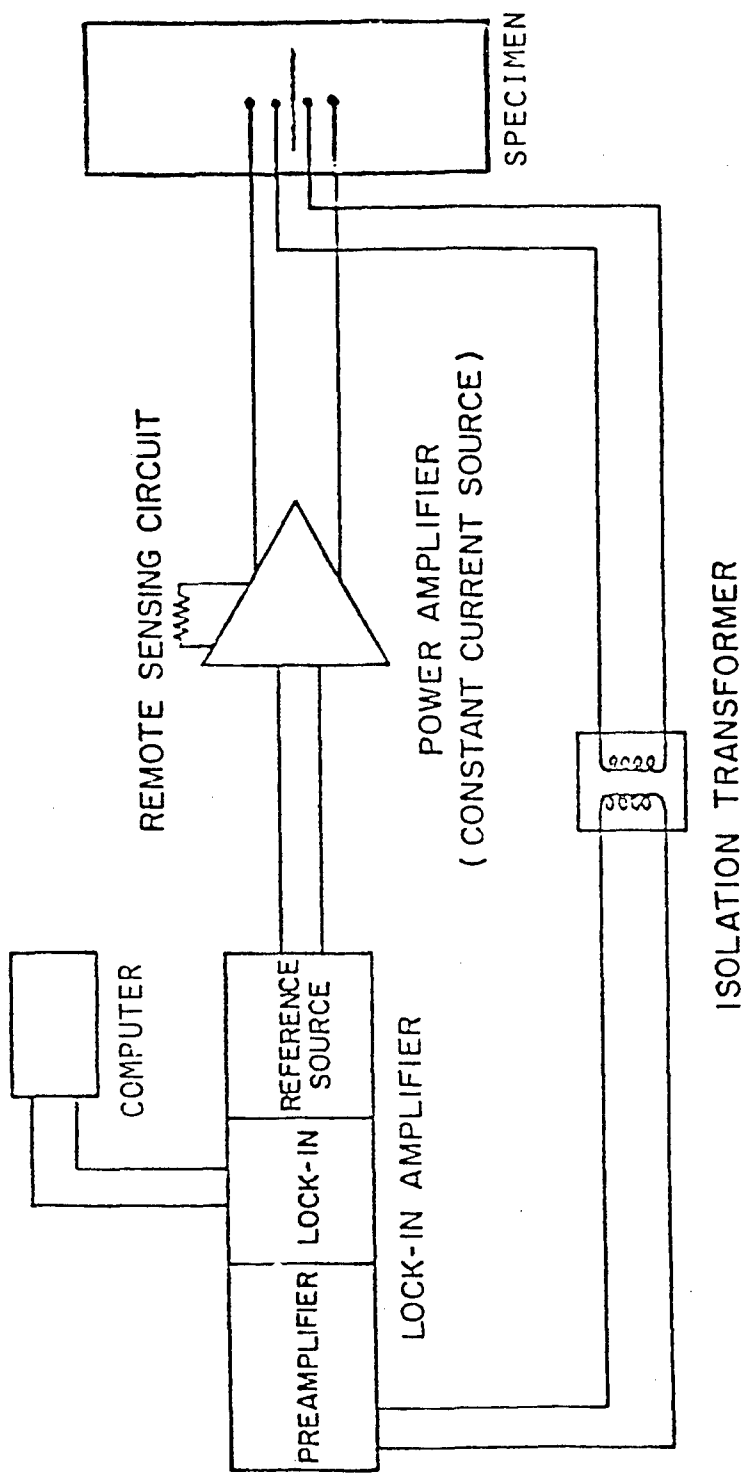
Figure 3. Block Diagram of the AC Potential System From Reference [8].

controlled stress intensity factor range (ΔK) for both the major and minor cycle components.

To maintain the appropriate test conditions, accurate crack length measurements were required. An empirical master curve of crack length versus normalized electric potential, shown in Figure 4, was determined for M(T) specimens. In initial applications, a constant normalized potential voltage V_0, determined at the start of the test, and the master curve were used to calculate crack lengths which allowed near real-time control of the test. Later, an updating scheme for V_0 was incorporated to modify the master curve whenever optical measurements of the crack lengths were made. The estimated crack lengths for the AC potential were within 5 to 10 mils of the optical crack lengths during the automated test.

2.5   THERMAL-MECHANICAL FATIGUE CRACK GROWTH

High temperature engine alloys typically see superimposed time varying temperatures and mechanical loads in service. A system was developed to simulate the mechanical and thermal service environment. The system is capable of providing combinations of in-phase, out-of-phase, combined in- and out-of-phase, and mixed frequency thermal and mechanical environments. The unit has been used to determine the effects of thermal/mechanical fatigue (TMF) loadings on the crack growth behavior of engine alloys.
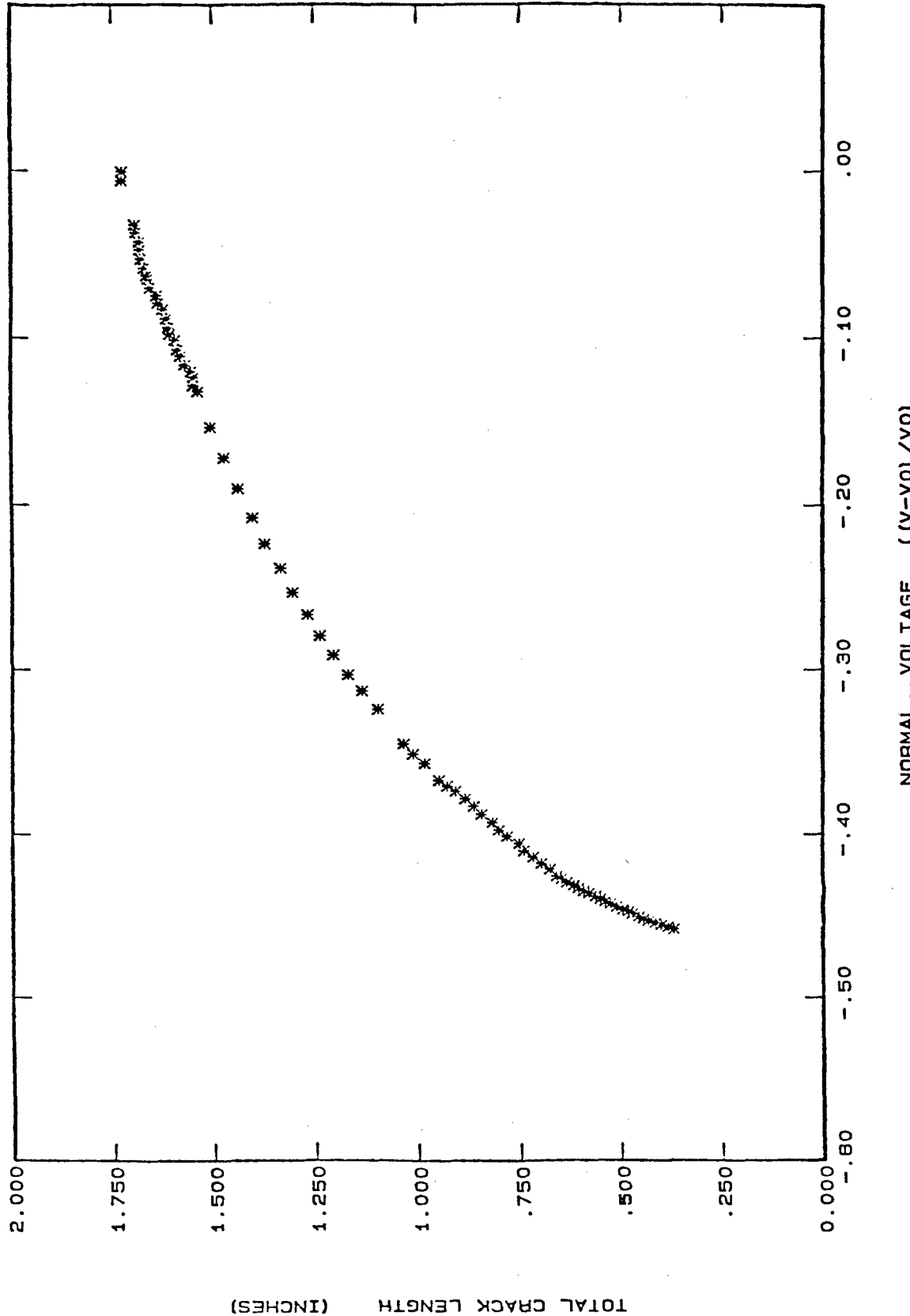
Figure 4. Normalized Electric Potential Curve for a CCT Specimen.

40

2.5.1 Control System: IBM 9000, Micricon

The major component of the system is an IBM System 9000 microcomputer which provides supervisory control, operator interface, data display, and data acquisition functions. A standard analog electronics package is used to control a servo-hydraulic test frame to apply the mechanical loads. A Research Incorporated Micricon 82300 industrial controller regulates the temperature. The Micricon has multiloop proportional/integral/derivative (PID) control capability and in the current configuration, four loops are used to control four independent temperature zones on the specimen [9]. The Micricon has an RS-232 serial interface which is connected to the IBM 9000. Information passes between the IBM and Micricon via the serial link to provide synchronization of the mechanical and thermal loading cycles.

To completely automate the system, some means of automatically measuring crack length was necessary. Several methods were reviewed including CMOD compliance and electric potential. Both methods are difficult to apply under nonisothermal conditions. Compliance would require nonlinear corrections for the changes in material modulus with temperature as well as thermal expansion corrections. The electric potential technique is sensitive to temperature

changes which cause material resistivity fluctuations and
thermal EMF voltages. Electric potential was eventually chosen
because compliance requires access to the crack region for
displacement measurement with an extensometer. The high
intensity quartz lamp (HIQL) system described below did not
allow sufficient space to install an extensometer.

2.5.2 HIQL Development

To gain an understanding of the crack growth
behavior under combined thermal and mechanical loadings
required the ability to simulate these conditions in the
laboratory. Closed-loop material testing systems capable of
accurately applying mechanical loads have been available for
some time. The remaining requirement was to develop a thermal
cycling system with sufficient speed and flexibility. The
system must be capable of rapid temperature excursions with
little temperature error and direct communication with the
mechanical load control system.

A new heating and cooling system was developed
which has the necessary capabilities. The system used quartz
infrared lamps to heat four independent temperature zones on
the specimen surface. Independent control of the four zones
maintained excellent temperature accuracy over the entire
region near the crack even during temperature cycling. The
quartz lamps were controlled by a microprocessor based Research

Incorporated Micricon 82300 industrial controller. This unit has the control and communication capabilities required to integrate thermal and mechanical cycling control functions.

Accurate cooling of the specimen during a thermal cycle was just as important as heating. The most common way to ensure controlled cooling was to design a cooling system to direct coolant evenly over the entire specimen surface. An alternate method was to adjust the coolant flow to attain a cooling rate higher than the desired rate and to allow the multizone heating system to provide makeup heat as required in each zone. The second approach was adopted and forced room temperature air was chosen as the coolant. The Micricon unit controlled a solenoid to start and stop the flow of the coolant and adjusted the lamp intensities to maintain the desired cooling rate.

2.6   HCF/LCF CAPABILITY

Three test systems for performing high cycle/low cycle fatigue (HCF/LCF) load conditions have been developed. Tests have been conducted in these systems at temperatures up to 1600F. Computer systems have been interfaced to these test systems to monitor and control the test. An Instron major/minor system provided high cycle load frequencies in the hundreds of Hertz and two other systems using MB C10 and C20 electromagnetic shakers generated load frequencies in the

kilo-Hertz range. A fourth test system was designed to provide tension-compression load conditions in contrast to the previous three systems which provide only tensile mean loads.

2.6.1   Improvements of HCF/LCF Systems

2.6.1.1   Instron System

Results of modal analysis studies of the Instron load train prompted the design of improved grips. The improved design availed more precisely repeatable alignment, more rigidity, and integral cooling which was required for elevated temperature tests.

An induction heater which had been used in earlier tests was initially replaced with a resistance furnace because of the susceptability of the Instron control electronics to the induction heater radiation. Now the furnace has been replaced with a quartz lamp heating system which allowed the use of shorter specimens and higher temperatures. The change to the quartz lamp system also provided the capability of thermal cycling - the temperature rise time being fast and the lamp controller being addressable by the computer.

2.6.1.2   C10 System

The frame of the C10 system has been improved with a stiffer cross member and a stiffer and better

alignable load cell. The induction heater has been replaced with a quartz lamp heating system. The simple timer has been replaced with a VIC-20 microcomputer allowing better operator control, safety interlocks, and potential for further automation.

2.6.1.3   C20 System

The C20 system is an automated and more powerful version of the C10 system. The C20 machine is capable of applying 10 kip low frequency loads and usable high frequency loads to over 1 kHz. It is interfaced to a VIC-20 microcomputer which has A/D and D/A converters for major and minor closed-loop load measurement and control as well as electric potential measurement of crack length. The system allowed a programmed loading profile rather than only a simple trapezoidal load waveform.

2.6.2   HCF/LCF Test System Performance Evaluation

At high frequencies, the test frame and specimen interact very strongly. A calibration procedure has been implemented wherein system load measuring equipment is calibrated by comparison with signals from strain gages located in the specimen gage zone. This calibration is intended for each specimen geometry and for each frequency range of interest.

High cycle fatigue tests can encounter many crack tip stress control problems arising from high frequency resonances in the specimen and load frame. Results from examination of the dynamic characteristics of the Instron major/minor machine for changing crack length and stress intensity in a M(T) specimen are discussed in Reference 10.

2.7 VACUUM SYSTEM FOR FATIGUE CRACK GROWTH TESTS

A vacuum chamber of nearly two cubic feet with a temperature capability to 2000F was designed and fabricated. A turbo-molecular pump has been utilized in the vacuum pump assembly in an attempt to obtain hard vacuum down to 10^{-9} torr. However, due to incorporation of rubber O-rings, ceramic support for heating elements, etc., a vacuum level around 10^{-5} torr would be achieved.

The vacuum system consisted of a stainless steel box with two large viewing ports to observe the crack length. Several other outlets for vacuum accessories as well as for pull rods which were attached to bellows were provided. The heating was achieved by Kanthal heating elements which were secured in another box split in two halves. The heating elements were backed by several layers of tantalum sheet which were designed for heat shielding. A large slot in each half of the heating

box assembly was provided to allow clear viewing of the specimen and crack length.

The vacuum system along with the furnace box was tested for leaks at room temperature. All the leaks detected were sealed and a vacuum of approximately 10^{-6} torr was obtained.

Vacuum dropped to a level of $5-6 \times 10^{-5}$ torr at 1200F during elevated temperature leak check. This was expected due to higher outgassing at elevated temperature. It is anticipated that an improved vacuum could be obtained by incorporating better cleaning procedures and low temperature baking, 200-400F, of the chamber from outside. Higher temperature baking is not possible due to the presence of rubber O-rings.

2.8   DEVELOPMENT OF LASER INTERFEROMETRY SYSTEM FOR
      INTERIOR OPENING OF A SURFACE CRACK

A simple Fizeau interferometer was developed to record and view the topology of a crack formed in an optically clear specimen. Laser illumination and pellicle beamsplitters provided improvements over earlier attempts to evaluate interior crack opening. High contrast fringes which were formed provided topographical information about the fracture surface in the loaded specimen.

The entire system is portable and is designed to mount on a sturdy tripod. Working distance and magnification are determined by simple changes in optics in the imaging system. Specimens can be prepared using both optically bonded flats to reduce distortion and antireflection coatings to reduce unwanted reflections.

The system was discussed at the 11th Annual Mini-Symposium on Aerospace Science and Technology, [11], and in a technical report, [12].

2.9   ACTUATOR SYSTEM FOR THE THETA RING

With the first Theta Ring prototype [13], major loading was achieved by manually torquing a nut in the load train. The major load was measured by a bridge of precision strain gages bonded directly do the Theta Ring. The second and third Theta Ring prototype designs incorporated a hydraulic actuator for the major loading. Since Theta is a resonance device, and symmetry of mass is a performance criteria, a suitable counterweight was machined integrally in the ring on the opposite side of the hydraulic cylinder mounting face. A standard 3 1/4 inch bore commercial cylinder was selected for the load actuator. With one of the cylinder end caps removed, it was bolted directly to the Theta mounting surface. The cylinder shaft was then made an integral end of the Theta load train.

For computer control of the hydraulic pressure in the actuator, a current-to-pressure (I/P) transducer was acquired from Scott Equipment Company. A hydraulic pump/reservoir package was also required from them. A VIC-20 computer has been planned to be dedicated to the I/P transducer as illustrated in Figure 5. As with the first prototype, strain gages bonded on the ring will provide the major load signal, but a pressure signal will also be monitored simultaneously. The well proven VIC-20 interface should adopt smoothly to this application; thereby, freeing an IBM 9000 for use in other applications.
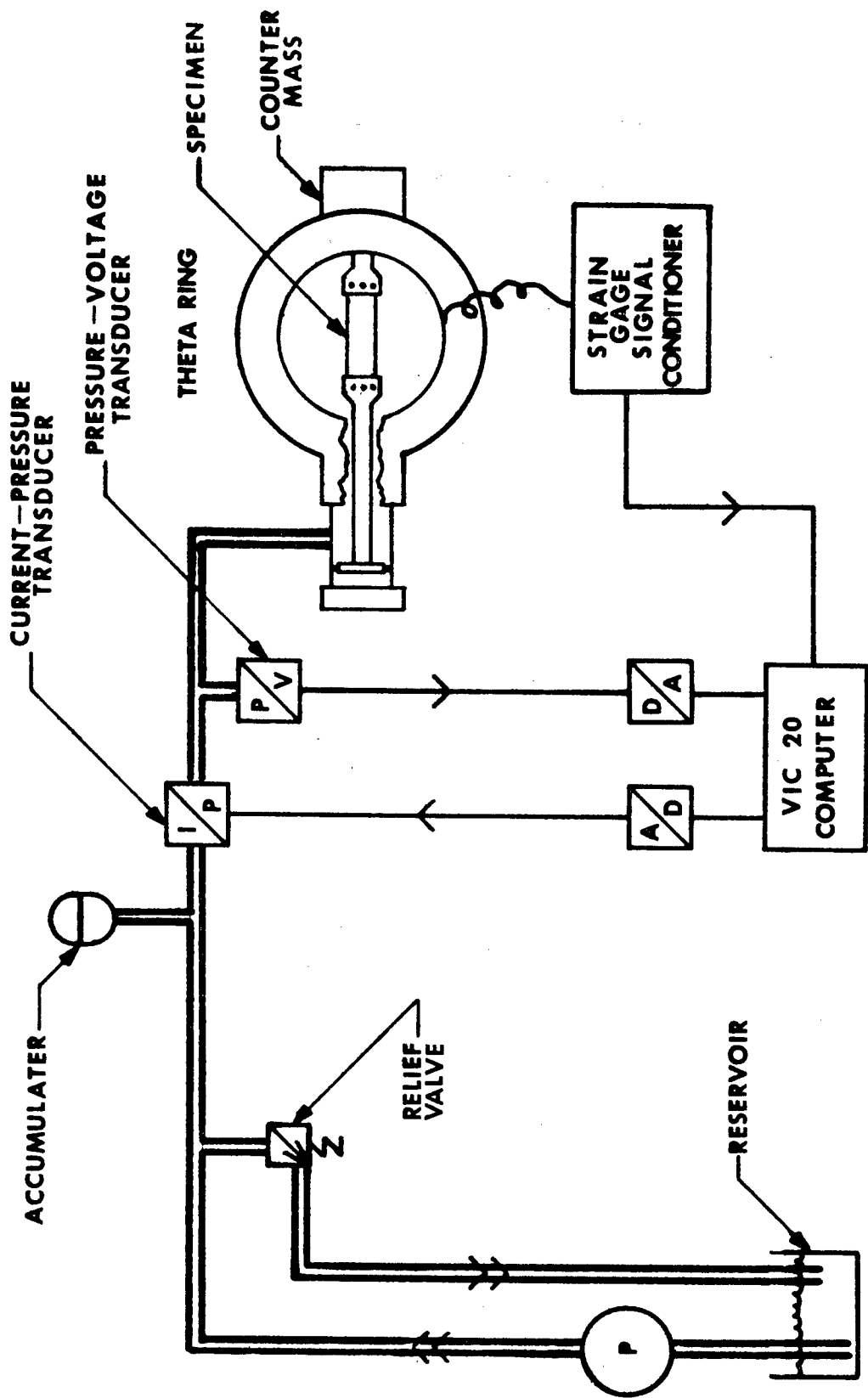
Figure 5. Theta II Major Load Control System.

SECTION 3

CRACK GROWTH CHARACTERISTICS

The ability to predict crack growth behavior in engine components is a key element for implementing the ENSIP requirements in future Air Force engine designs. In attempts to understand and model the growth characteristics, the crack growth behavior of a variety of engine materials was studied over a wide range of temperatures and load histories. Studies of the influence of environment on the sustained load crack growth behavior were also conducted. This section describes the test results and analyses of crack growth investigations conducted under this program.

3.1   CREEP FATIGUE INTERACTION

3.1.1   Crack Growth as a Function of Frequency,
         Temperature, Stress Ratio, and Stress Intensity
         Factor

Numerous investigations report that the crack growth rate (CGR) in nickel-base superalloys is governed primarily by the frequency, temperature, stress intensity factor, and load ratio. Depending on the frequency and temperature which can produce a combination of environmental

51

and creep effects, CGR can be characterized in the range between fully time-dependent component behavior and fully cycle-dependent behavior.

In these investigations, the CGR behavior of two nickel-base superalloys, Inconel 718 and Gatorized IN100, were studied as a function of temperature and frequency. All tests were conducted at constant maximum stress intensity factor of either 25 or 40 MPa$\sqrt{m}$. The tests were divided into two types. In one series of tests, frequency was kept constant while the crack was grown for blocks of cycles at different temperatures. In the other series of tests, the temperature was held constant while the crack was grown in blocks of cycles at various frequencies. The stress ratio, R, was maintained at 0.1 for all tests and a triangular waveform was used throughout the test program.

All tests were conducted using a servo-controlled hydraulic test machine and a microcomputer. Crack lengths were monitored from compliance calculations based on CMOD measurements obtained from a high temperature clip gage with quartz extension rods. Additionally, a DC electric potential system was used to obtain crack lengths at higher frequencies. As the crack grew, loads were changed by the computer control to maintain the desired stress intensity factor (K) history. A resistance furnace surrounding the specimen was used to maintain temperature.

CGR was obtained using a least square minimization technique once a steady state growth rate was achieved for each condition of temperature and frequency. Crack lengths were later verified by comparison with the fracture surface markings. The fracture surface was analyzed using an optical microscope and scanning electron microscope for the identification of various micro-mechanisms of crack length.

The CGR as a function of temperature is plotted for three different frequencies for Inconel 718 in Figure 6. For a given frequency, the CGR increases with temperature above 430C (800F); and below this temperature the CGR is observed to be basically independent of both temperature and frequency and becomes fully cycle-dependent. Similar observations were made for IN100 where the transition temperature was approximately 500C. Figure 7 shows the CGR as a function of frequency for Inconel 718 at 649C (1200F) and $K = 40$ MPa$\sqrt{m}$. At 649C, the CGR of Inconel 718 increases with decreasing frequency. If the CGR data of Figure 6 are plotted a time rate of growth (da/dt), it is observed that a frequency exists below which the da/dt is approximately constant. Below this frequency, the CGR is assumed to be fully time-dependent. For IN100, over the range of temperatures studied, there was no indication of a transition frequency for fully time-dependent behavior.
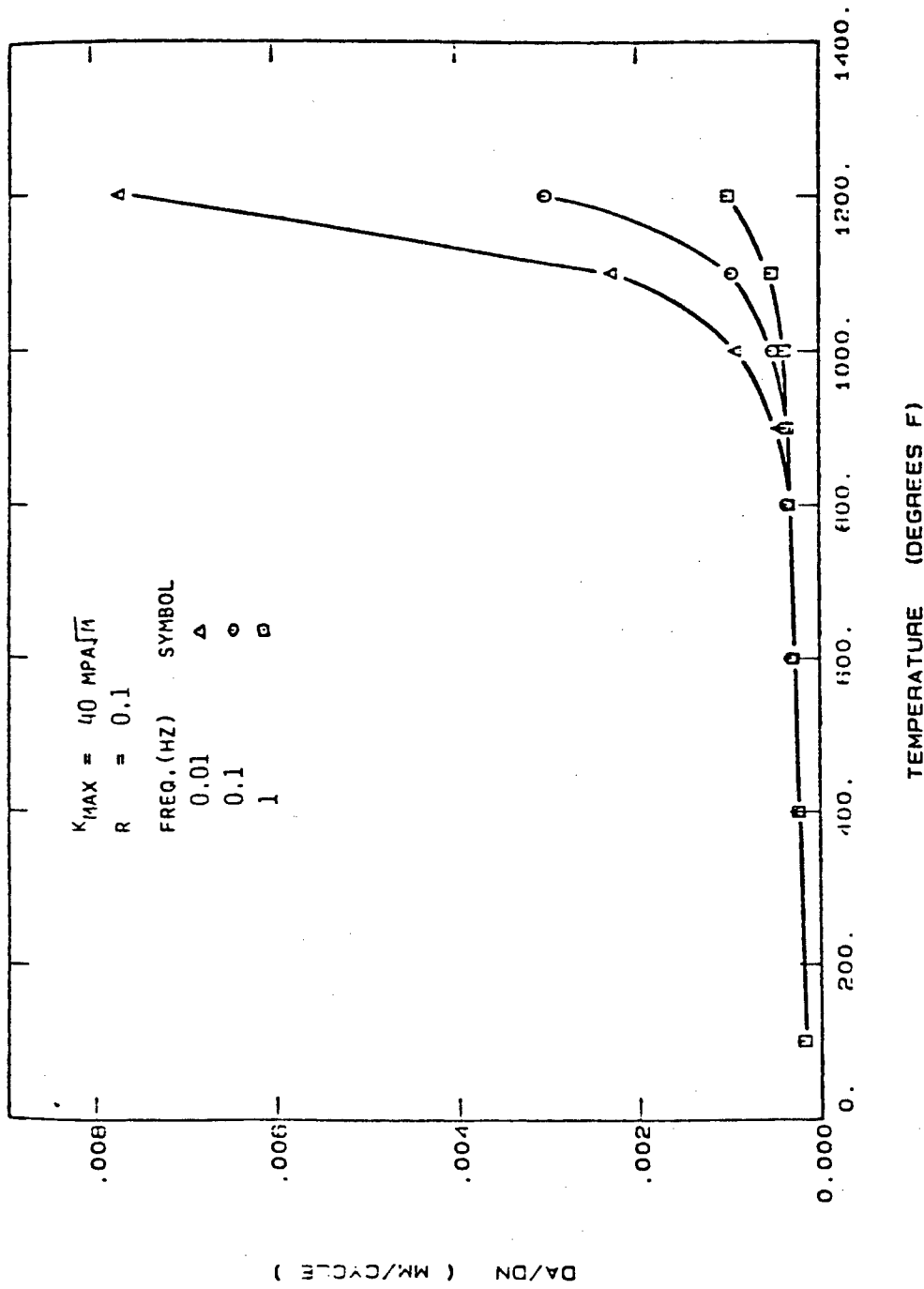
Figure 6. CGR as a Function of Temperature at .01, 0.1, and 1.0 Hz for IN718.

54
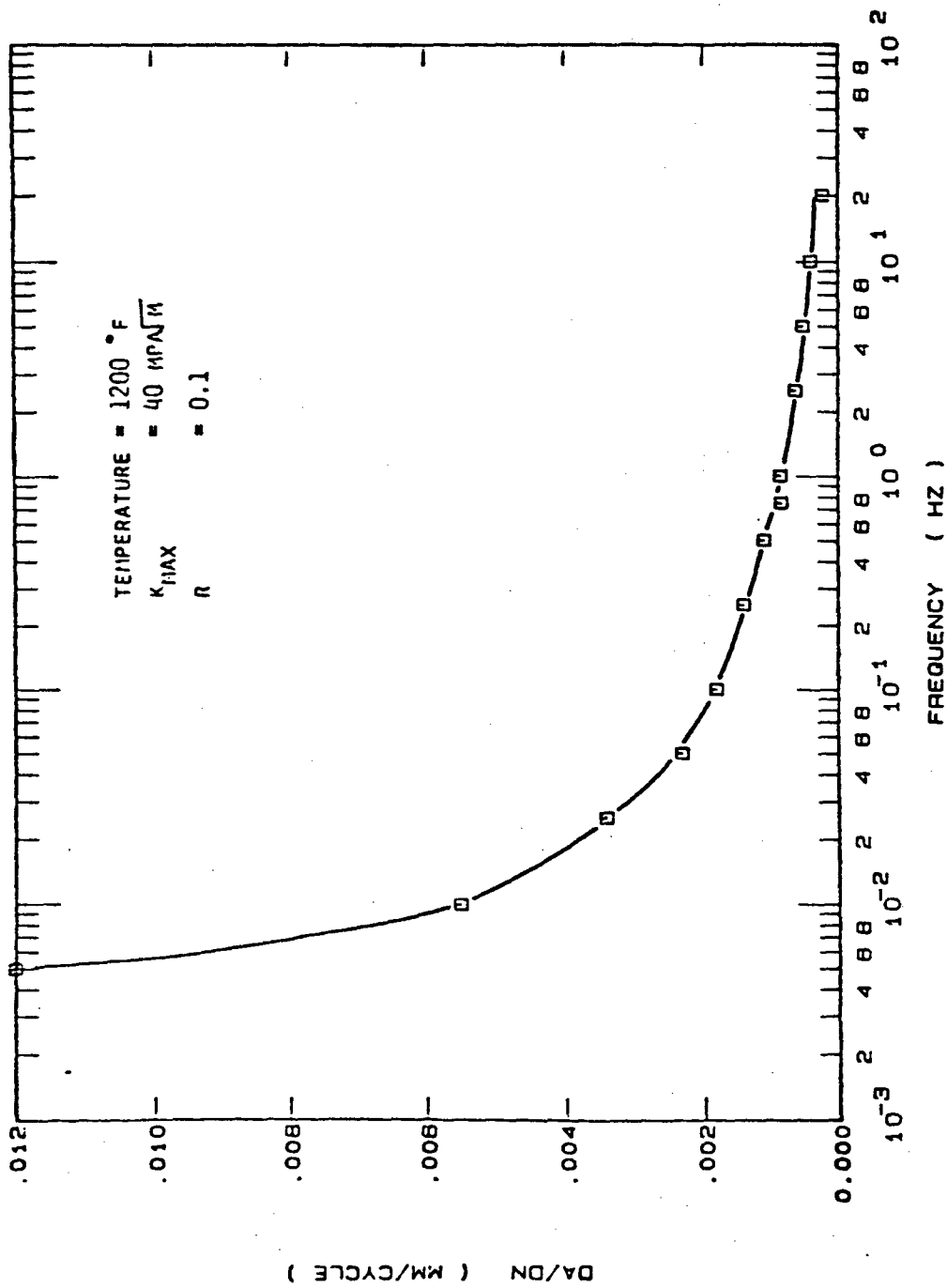
Figure 7. CGR as a Function of Frequency at 650°C (1200°F) for IN718.

55

The CGR can be considered as consisting of two components: a fully cycle-dependent fatigue component and a fully time-dependent component. CGR modeling was performed using this concept. In the model, the transition from fully cycle-dependent to mixed-mode behavior and from mixed-mode to fully time-dependent behavior is based primarily on frequency. In addition, CGR maps were constructed based on the cycle-, mixed-, and time-dependent basis. Micro-mechanistic observations were also included in the maps. Test techniques and modeling were discussed in detail in Reference 14.

Fatigue crack growth rate of IN718 and IN100 were studied as a function of temperature and frequency at constant stress intensity factors also. Fatigue crack growth was observed to increase as a function of increasing temperature or decreasing frequency. A model was developed to characterize the growth rate as the sum of a cyclic component and an effective time-dependent component. The details of the model are described in Reference 15.

3.1.2   Hold-Time Effects in Elevated Temperature
         Fatigue Crack Propagation

An experimental investigation was conducted to evaluate the effects of hold-time on the fatigue crack growth rate of Inconel 718 at 649C using compact type

specimens. Tests were run under computer-controlled constant-K conditions using compliance to determine crack length. Hold-times ranging from 5 to 50 s were applied at maximum, minimum, and intermediate load levels. The data implied that hold-times at maximum load were the most damaging in terms of increased crack growth rate. Hold-times greater than 5 s led to purely time-dependent crack growth behavior which was predictable from sustained load data using K as a correlating parameter. Hold-times at minimum or intermediate load levels had little or no effect on crack growth rate. A linear cumulative damage model based solely on fatigue and sustained load data was found to be adequate for spectrum loading as long as the hold-times were at maximum load. The model is described in Reference 14.

3.1.3 Micro-Mechanisms of Crack Growth in Creep/Fatigue Interaction

Micro-mechanisms of fatigue crack growth were studied in nickel-base superalloys, IN718 and IN100, as a function of temperature and frequency at constant stress-intensity-factor conditions. Temperature and frequency were varied from 20 to 648C and from 0.001 to 10 Hz, respectively.

Crack growth rates were determined and fractography observations were made from test specimens. It

was determined that micro-mechanisms of fatigue crack growth rate are a function of temperature or frequency for a given K value. With decreasing frequency, the crack growth mechanisms changed from transgranular to intergranular failure. Also, with increasing temperature, the mechanisms of growth changed from transgranular to intergranular failure. These results were presented in Reference 16.

3.2   HCF/LCF BEHAVIOR

The effects of combined high cycle and low cycle fatigue (HCF/LCF) on gas turbine components have posed a potential problem in estimating the life of the components. For damage tolerance evaluation, the effects of HCF/LCF on crack propagation must be determined. An earlier investigation into this problem is described in Reference 10. An HCF/LCF load cycle, shown in Figure 8, is annotated in terms of the stress intensity factor and some other pertinent terms.

Data have been generated from C(T) and M(T) specimens of Inconel 718 under various load, frequency, and isothermal conditions:

$$\Delta K_{maj} = 15, \ 20, \ 25, \ 30, \ 35, \ 40 \ \text{MPa}\sqrt{m},$$

$$R_{maj} = 1 - \Delta K_{maj}/K_{maj} = 0.1,$$
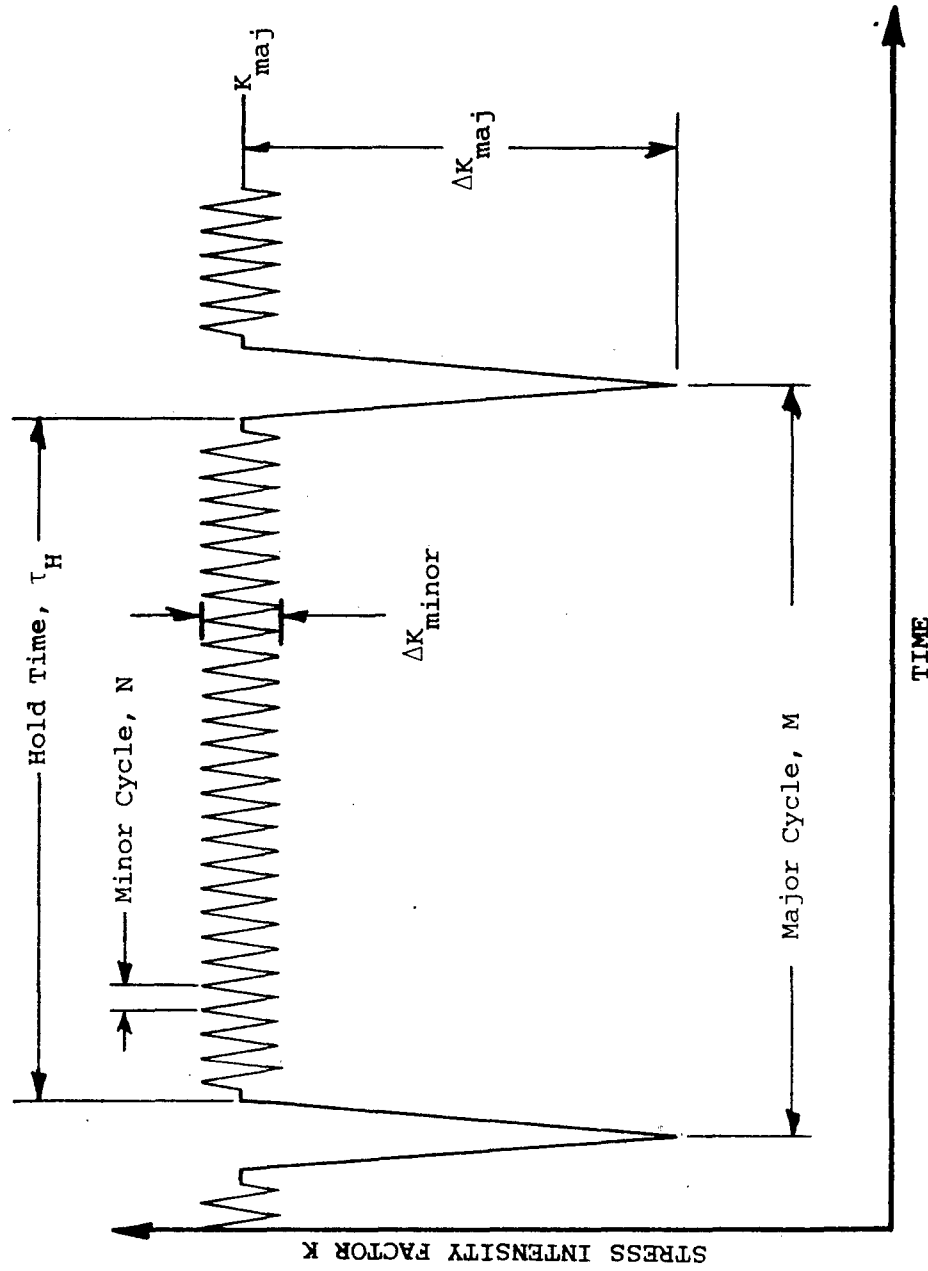
Figure 8. An HCF/LCF Load Cycle.

59

$$0 \le \Delta K_{minor} \le 60 \text{ MPa}\sqrt{m},$$

$$\tau_H = 60, \ 180, \ 600 \text{ s},$$

$$\nu_{minor} = 10, \ 100 \text{ Hz}$$

$$T = 24, \ 538, \ 649C$$

Some of the results of these tests are shown schematically in Figure 9. The crack growth rate was found to depend upon major cycle stress intensity factor, ΔK_{maj}, hold-time, τ_H, and minor cycle frequency, ν_{minor}, and stress intensity range, ΔK_{minor}, for a given temperature. The elevated temperature tests also demonstrated a transition from creep crack growth dominant to fatigue crack growth dominant at values of minor cycle amplitude above a threshold value.

Further discussion of the results under this effort is given in References 17-20.

3.3 CREEP CRACK GROWTH (CCG) IN LABORATORY AIR

It is important to determine the principal parameters which govern the crack growth behavior in nickel-base super-alloys at elevated temperatures under sustained loads. These parameters provide a better understanding for the development of crack growth models which improve the capability of
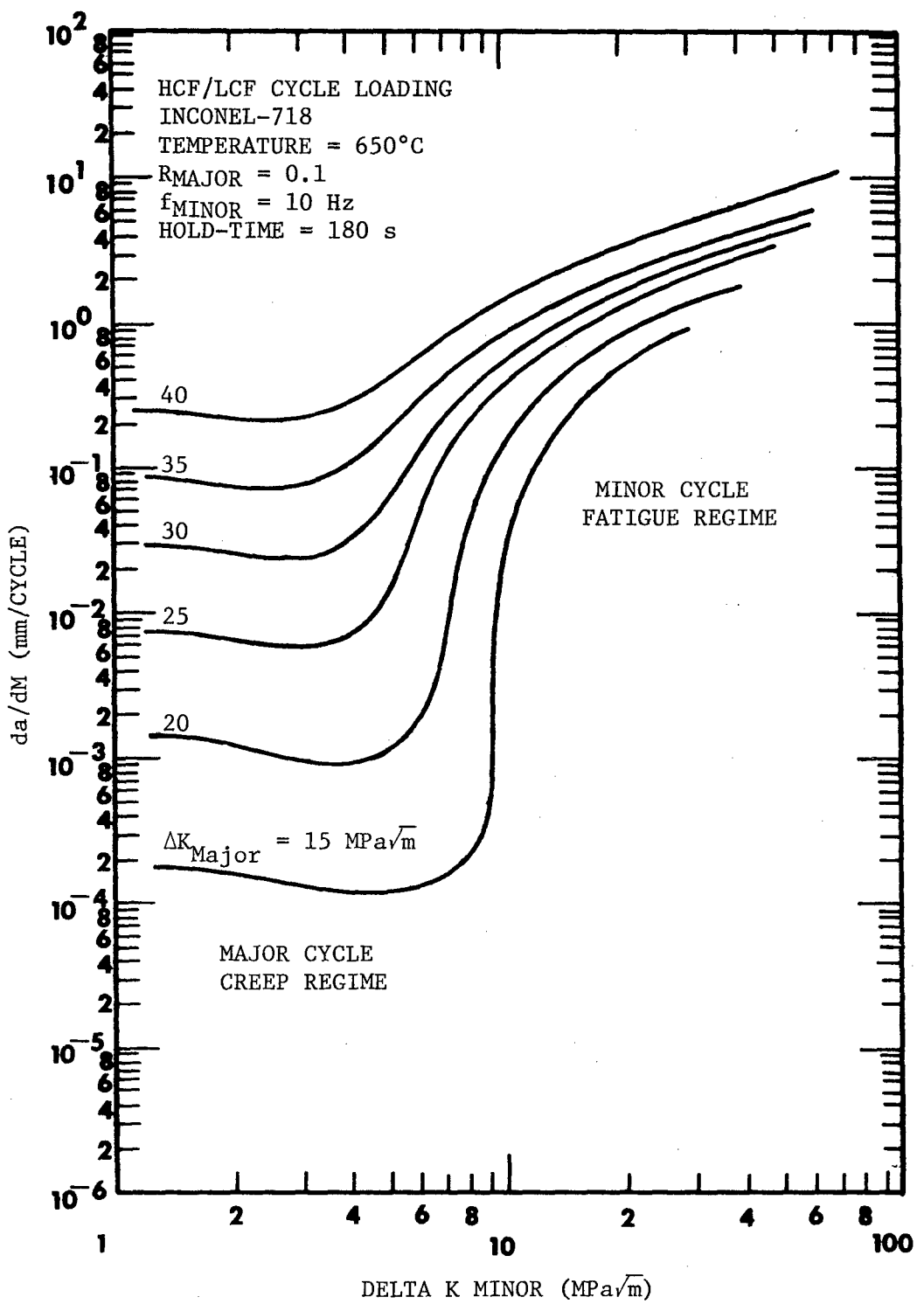
Figure 9. Crack Growth Rate as a Function of ΔK_{Minor} for Various ΔK_{Major}.

predicting crack growth in materials which are used under
extreme operating conditions such as those produced in gas
turbine engines.

3.3.1   CCG in IN100

Crack growth behavior was investigated in a
nickel-base superalloy (IN100) at 732C in laboratory air under
sustained load. The tests were conducted on side-grooved
compact type specimens. One purpose of this study was to
evaluate the effect of the through-the-thickness stress
distribution upon crack growth behavior in grooved specimens.
Also in this study the effects of crack orientation and net
thickness between the side-grooves were evaluated.

The crack growth rates as a function of stress
intensity factor showed only a slight dependence upon thickness
and were independent of crack orientation. Also, the growth
rates at the same stress intensity level in the grooved
specimens were faster than the rates in the smooth specimens,
which indicated that the "plane-stress region" near the sides
of the smooth specimen tends to retard the crack growth in the
interior of the specimen. A model for the crack growth rate
as a function of stress intensity factor and a more detailed
discussion of the results can be found in Reference 21.

3.3.2 CCG in IN718

In a gas turbine engine, components undergo a constant load for a period of time at elevated temperatures. Some of these components are critical in the determination of the life of the engine. In order to predict the durability and safety of the engine, it is necessary to determine the behavior of crack growth in materials of the critical component.

The objective of this investigation (reported in Reference 22) was to determine baseline crack growth rate data for IN718 at elevated temperatures under constant load. These data would be subsequently used in the development of life-prediction models. One aspect of the investigation was to determine if specimen geometry has an effect on the creep crack growth rates in IN718 under the test conditions. Specimens were fabricated from plate and sheet stock of IN718. Specimens from both plate and sheet stock received the same standard heat treatments.

Four in-plane geometries -- compact tension (C(T)), single edge notched (SE(T)), single crack ring tension (SCRT), and an arc-shaped specimen (MC) -- were tested from the plate stock. The crack was located in the TL orientation for the C(T), SE(T), and SCRT specimens and in the LT orientation for the MC specimen. Three thicknesses of C(T)

specimens were tested where one of the thicknesses was associated with a specimen having one-half the in-plane size of the typical specimen. Two in-plane geometries -- M(T) and C(T) -- with cracks in the TL and LT orientations were tested from the sheet stock. All specimens were precracked at room temperature and the maximum stress intensity factor at the final precrack length was always less than the initial stress intensity level for the test. The test temperature for most of the crack growth data was 649C (1200F) with some data being collected at 593C (1100F), 538C (1000F), and 482C (900F).

Crack growth data, da/dt, from the four specimen types at 649C from the plate stock agreed within a reasonable scatter. No variations in the data were noted for changes in thickness or for the change in in-plane geometry. However, a change in growth rate was observed for a specimen from another batch of material. The growth rate which was a factor of two higher than in the original batch could not be attributed to heat treatment.

The growth rate in the sheet material was also significantly higher than in the plate material. Growth rates from both specimen geometries were in agreement at 649C. Crack orientation did not have a pronounced effect on the growth rates.

Loading history did effect the crack growth rates. The greatest impact of prior loading occurred at the very slow growth rates where small overloads stalled the crack growth. An attempt was made to model the crack growth in both the transient and the steady state phases.

As part of the previous observations, the following conclusions were reached from this investigation:

a. The stress intensity factor is an adequate parameter to characterize steady state creep crack growth in IN718 at 649C.

b. Previous loading history can create transient crack growth behavior which significantly affects the total life and which is not directly related to the stress intensity factor calculated from remote loads.

c. Greater variations in crack growth between batches of material occurred under creep conditions than under fatigue conditions.

3.4 ENVIRONMENTAL EFFECTS ON CRACK GROWTH BEHAVIOR

In the past decade, research on the significance of the environment in fatigue and creep behavior of high

temperature alloys has clearly demonstrated the need for a better understanding of its influence on mechanical behavior for a meaningful approach to life-prediction modeling.

Since the environmental effect is a phenomenon which is dependent on time, temperature, and stress parameters, the interaction which takes place between the chemical processes and mechanical effects of the applied load, which involve frequency, load amplitude, and waveshape as variables, must be characterized by all the above parameters. In a simple approach, the influence of single parameters can be initially studied and the results can later be used in modeling the interactions of several parameters.

To isolate the effect of environment on the elevated temperature mechanical behavior of materials, crack growth tests were conducted on IN718 and nickel-base superalloy single crystal N4 in both laboratory air and a vacuum of approximately 10^{-6} torr.

Tests were also conducted to study the influence of hot corrosion on nickel-base alloy Rene' 77 and Rene' 80 to understand the influence of more realistic engine environment. This effort was further extended to the study of the effect of hot corrosion on mechanical behavior such as creep rupture. The following section deals with the procedures, test results, and analysis of these tests.

3.4.1 Effect of Environment on Creep Crack Growth (CCG) in IN718

The influence of the most common environment -- the atmosphere -- on the CCG of IN718 was investigated by studying the CCG behavior of this alloy in both laboratory air and a vacuum of approximately 10^{-6} torr.

Creep crack growth tests were conducted on IN718 in the temperature range of 538C to 704C to investigate the influence of environment on elevated temperature crack growth behavior. Creep crack growth rates at 649C were found to be over two orders of magnitude higher in laboratory air than in vacuum. The fracture was found to be intergranular at 649C in air, while it was transgranular in vacuum [22]. At the higher temperature of 704C, the creep fracture was intergranular even in vacuum. It appears that the partial pressure of oxygen at a specific temperature for a particular alloy plays a dominant role in controlling the mode of failure.

3.4.2 Effect of Environment on CCG in Rene' N4 Single Crystal

The crack growth behavior of N4 single crystal under sustained load was investigated in laboratory air and vacuum environments. Since the material was a single crystal, the effect of crystal orientation was also evaluated.

The notation [001]/[100] means that the unloading axis is [001] direction while the crack front grows parallel to [100] direction. The casting property of the single crystal leads to two situations along the crack front direction. The crystals, although oriented in [100] direction for crack propagation may have the primary dendrite either aligned parallel to [100] or perpendicular to [100].

CCG tests were conducted with specimens oriented in such a way that (a) the crack front was parallel to primary dendrite direction and (b) the crack front was perpendicular to primary dendritic arm.

3.4.2.1 CCG in Rene' N4 Single Crystal [001]/[100] Orientation in Laboratory Air

These tests were conducted on subcompact type (W = 20 mm) specimens at 1600F and 1800F.

Precracking of these specimens posed some problems. Initially, the precracking was conducted at room temperature. Various frequencies were tried but the cracking mainly initiated at or near the notch root and continued at nearly 45° to the plane of symmetry.

The problem of precracking N4 single crystal was solved to some extent by precracking the specimen at elevated temperature. Several combinations of temperature and frequency were tried. Relatively good results were obtained at 1000F and 20 cpm, which has been adopted as a routine procedure for precracking N4 single crystal.

Two sustained (constant) load tests were conducted at 1600F and two at 1800F. The stress intensity was varied from 20 ksi$\sqrt{in}$ to 40 ksi$\sqrt{in}$ at 1600F and from 15 ksi$\sqrt{in}$ to 40 ksi$\sqrt{in}$ at 1800F. The load was increased in steps of 10% to achieve higher K values at intervals of 40 to 50 hours. No growth was observed even after 100 to 150% increase in the values of K. In all these cases, tremendous crack tip blunting occurred and net section creep was observed. As a result, no CCG data could be obtained and it was decided to use side-grooved specimens for future tests.

CCG tests on side-grooved subcompact specimens were conducted at 1600F and 1800F. Initially, the tests were conducted on side-grooved precracked specimens having a/W = 0.4. Even this long precrack did not result in high enough K under the load capability of grips and pins. Long exposures at loads equivalent to 30 ksi$\sqrt{in}$ at 1600F resulted in crack tip blunting as well as creep of grips and pins.

The design of the grip as well as the loading pins could not be modified easily, largely due to the restriction imposed by the specimen geometry.

Hence, the tests were conducted on specimens precracked to crack lengths with a/W as high as 0.53. The results are shown as plots of crack length vs time and da/dt vs K in Figures 10 through 13.

The fractured specimens were observed under an optical microscope followed by an SEM. The fracture surfaces observed at 1600F and 1800F were mainly interdendritic and mode I failure was predominant over the creep zone which changed to mode II in the fast fracture zone as shown in Figure 14.

3.4.2.2 CCG of Rene' N4 Single Crystal
         [001]/[100] Orientation in Vacuum

Similar problems of load restriction due to grip design occurred in the vacuum tests as in the laboratory air tests. Other problems were encountered that inhibited progress included those with: (a) the extensometer and vacuum chamber cooling systems, (b) the heating panels and controls, and (c) the vacuum pumps. These problems were resolved. Tests are planned on long precracked specimens with a/W approximately 0.53.
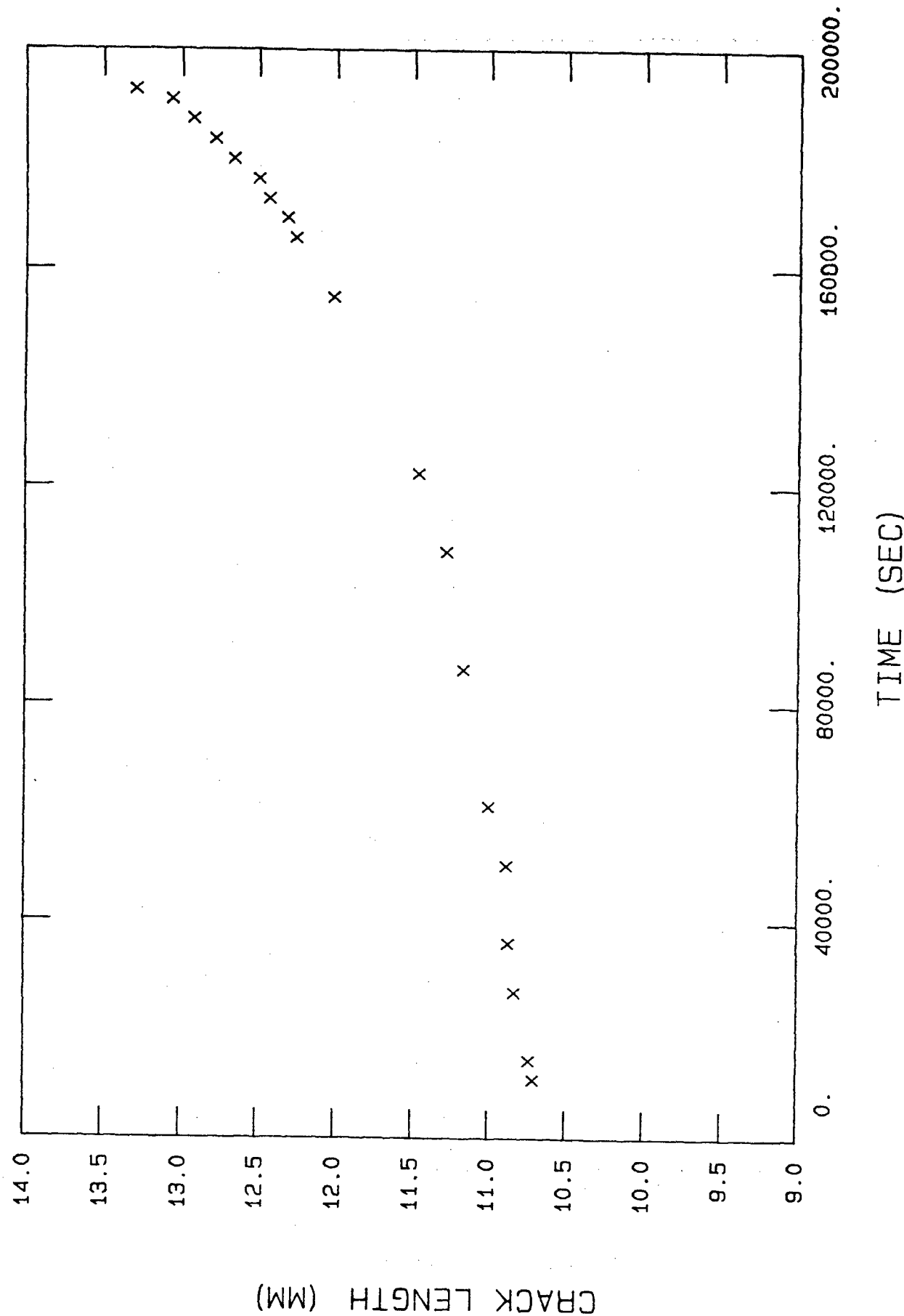
Figure 10. Crack Length vs. Time for a Rene' N4 Single Crystal Tested at 1600°F.
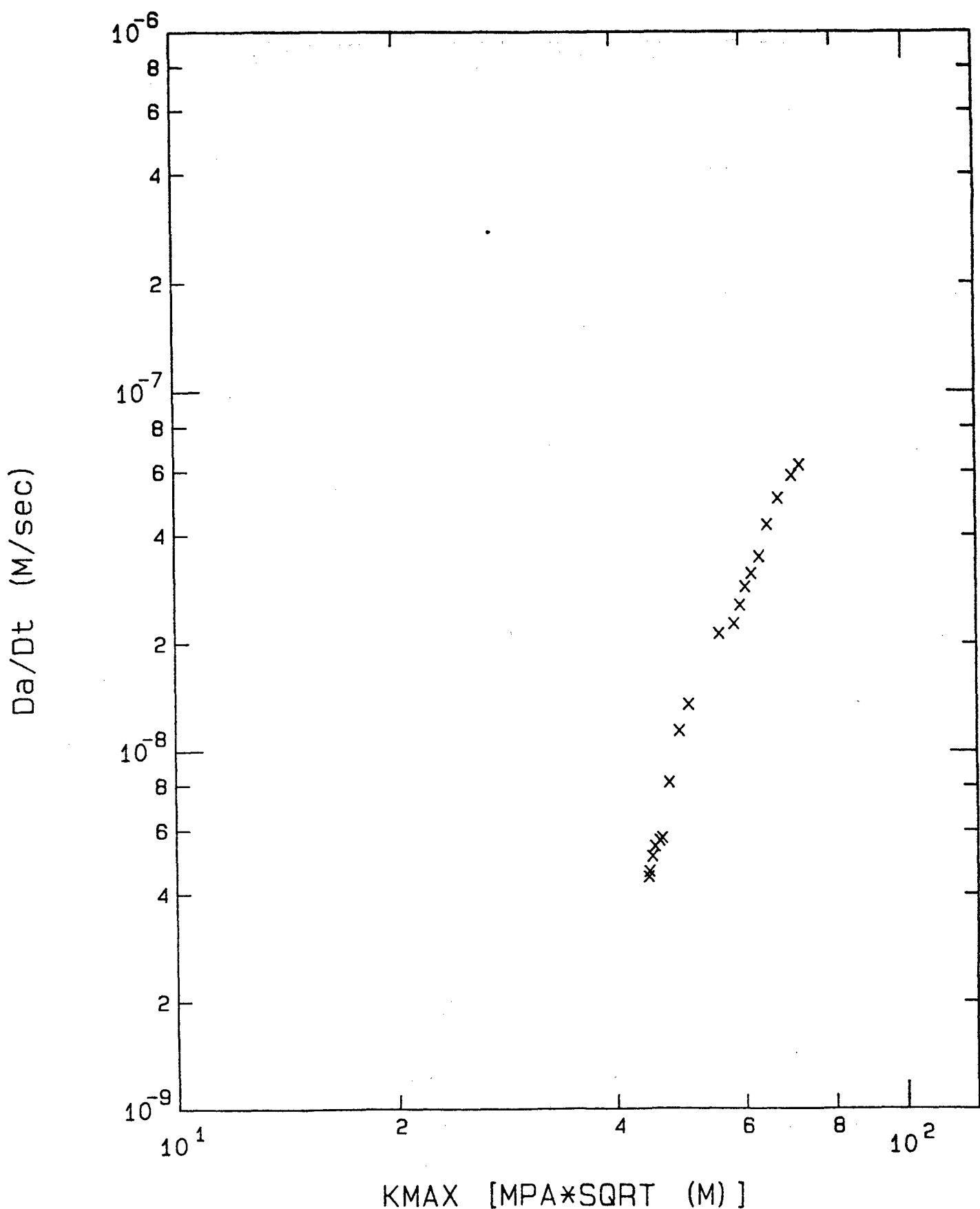
Figure 11. K_{max} vs. da/dt Behavior for Rene' N4 Single Crystal
   Tested at 1600°F.
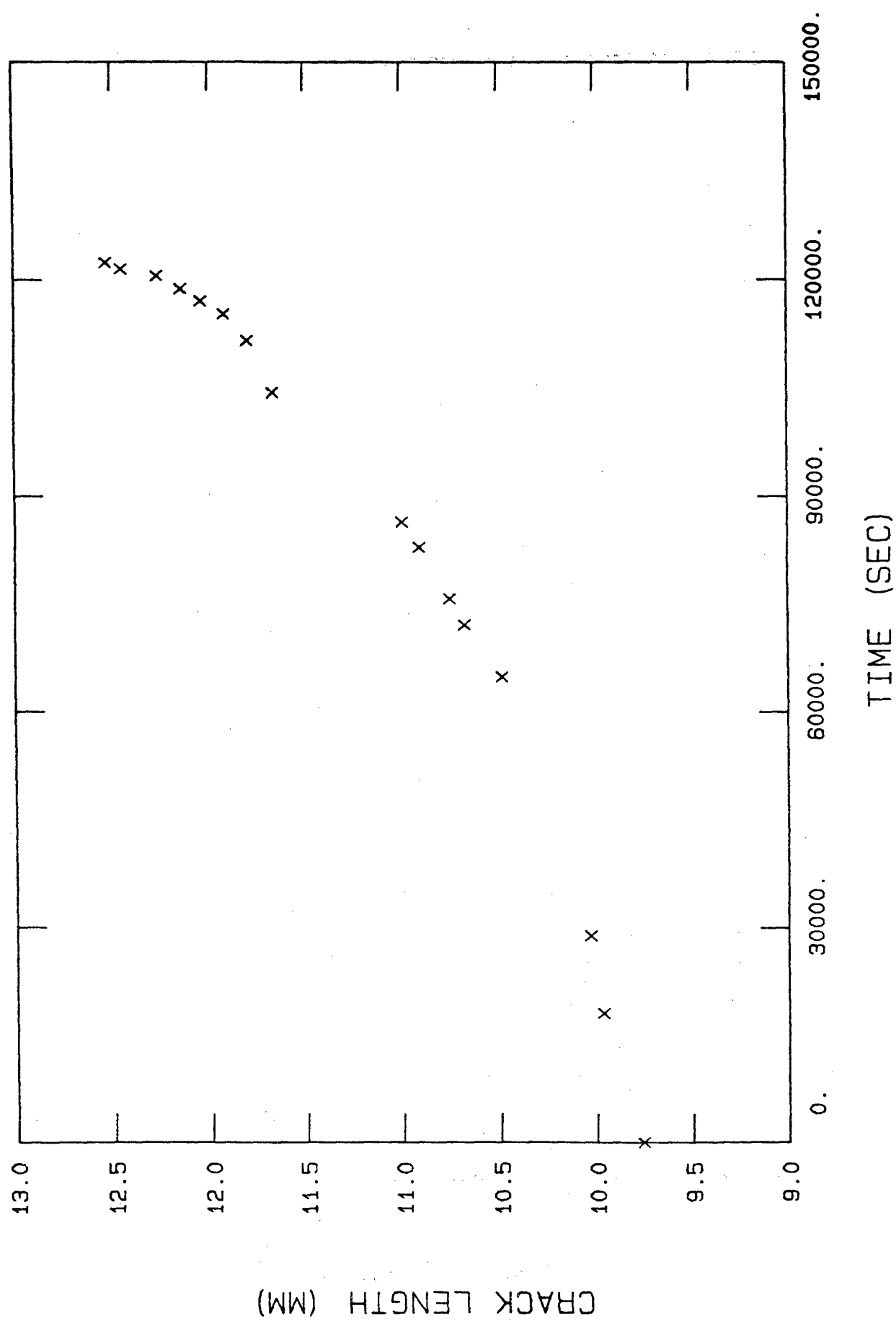
Figure 12. Crack Length vs. Time for a Rene' N4 Single Crystal Tested at 1800°F.

73
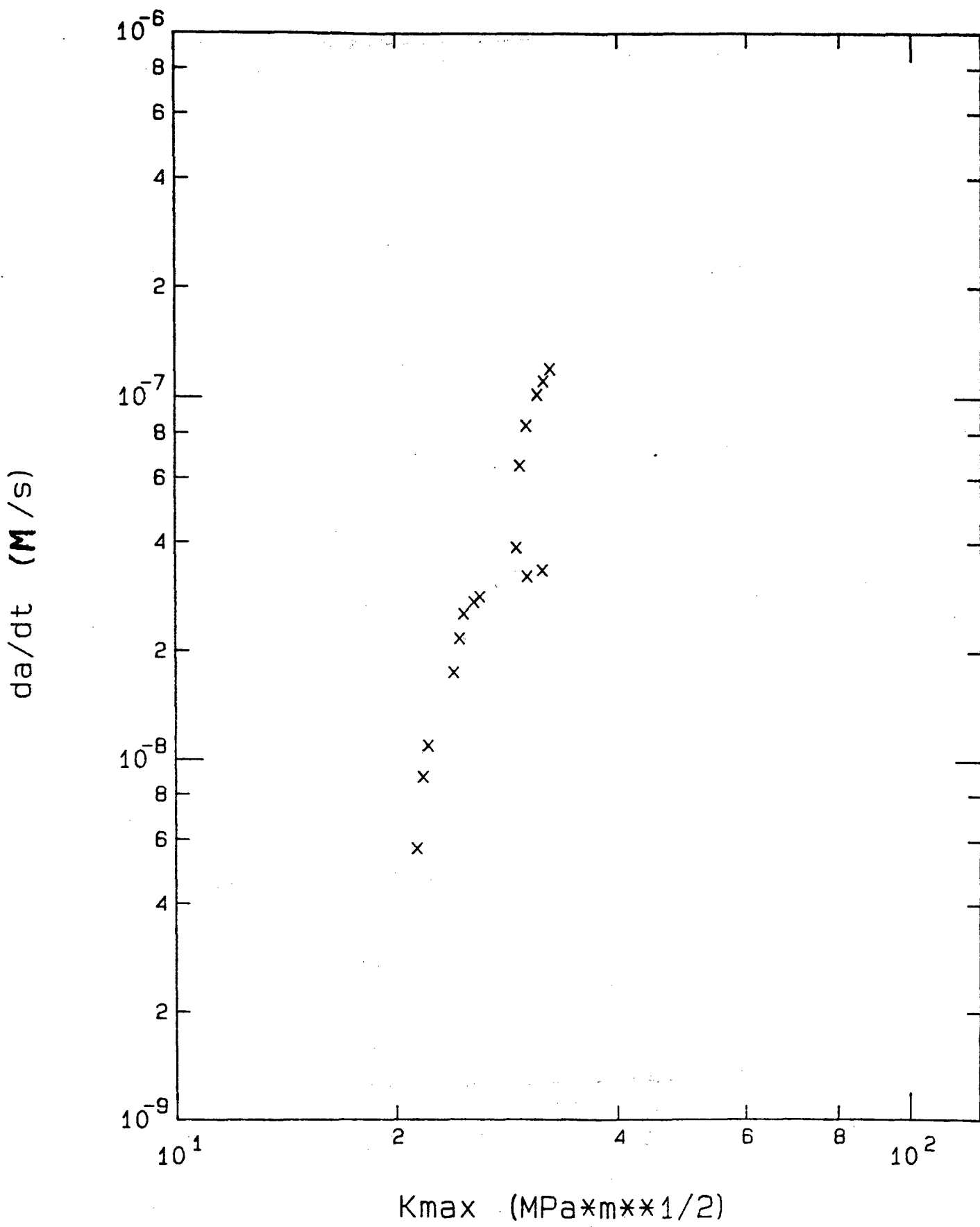
Figure 13. K_{max} vs. da/dt Behavior for Rene' N4 Single Crystal Tested at 1600°F.
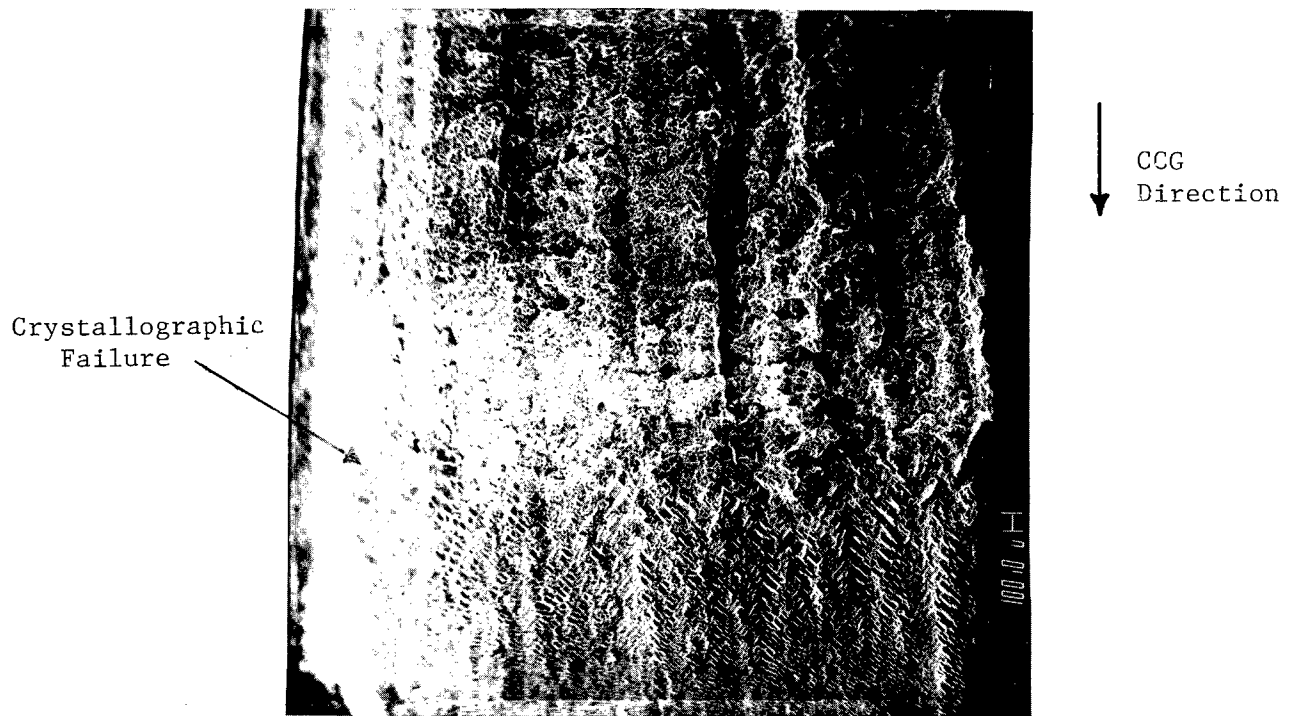
Figure 14. Low Magnification View of Fractured Surface of
Rene' N4 Single Crystal Tested at 1800°F.

3.4.3 Creep Rupture on N4 Single Crystal Oriented in [001] Direction

Tests were conducted at 1400F and 100 ksi. The fractured surface showed evidence of microporosity and some evidence of crack initiation from such micropores. The general features of fracture surface tested at 1400F is shown in Figure 15.

3.4.4 Fatigue Crack Growth of N4 Single Crystal Oriented in [001]/[100]

Nickel-base superalloy single crystals such as Rene' N4 have great potential as turbine blade materials for high performance aircraft. These single crystals possess an excellent combination of mechanical properties and corrosion resistance. Detailed information on the mechanical or crack growth behavior properties of these alloys is lacking. Such information is a prerequisite for any life-prediction modeling of turbine blades. An extensive program was initiated to study elevated temperature fatigue of Rene' N4 single crystal alloy. The objective of the program was to understand the influence of environment and effects of anisotropy on high temperature fatigue properties.
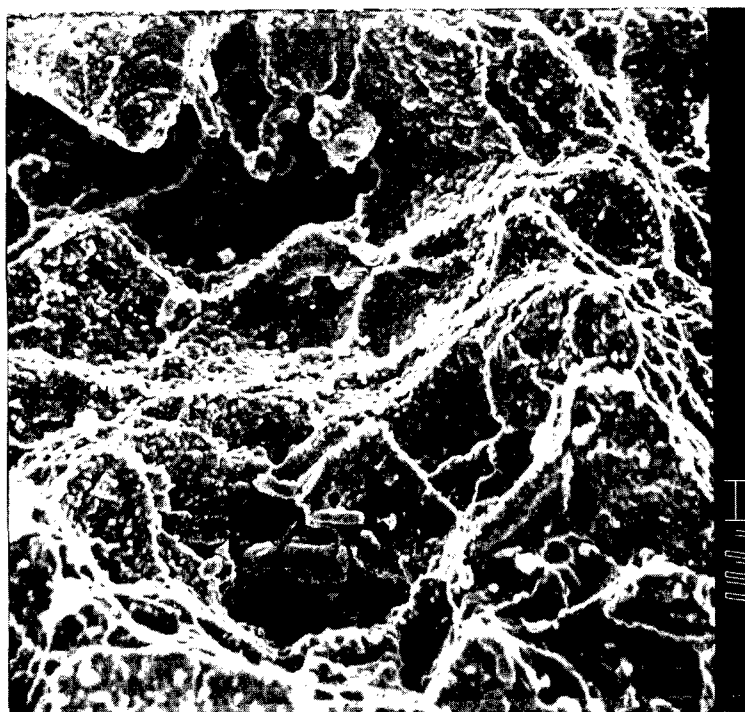
Figure 15. General Feature of Creep Rupture Surface of
Rene' N4 Single Crystal at 1400°F.

Constant load fatigue crack growth tests were conducted over a wide range of temperatures from 1000F to 1600F. C(T) specimens, W = 20 mm and B = 5 mm, were utilized for most of the testing. Other C(T) specimens, W = 40 mm and B = 10 mm were also used to study the effect of specimen thickness. Two crack growth orientations, [100] and [110] with [001] as tensile axis, were tested to investigate the effect of anisotropy. Experiments were conducted at test frequencies of 20 and 60 cpm.

Fatigue crack growth in these two orientations were found to be similar in the central power law region at temperatures between 1000F and 1200F, at both frequencies tested. In all cases, the crack growth occurred in two distinct modes. At low stress intensities, mode I cracking with a rough fracture surface was observed. This resolved into dimple morphology at higher magnification. Whereas, at higher stress intensity levels, a mixed mode (mode I and mode II) faceted and crystallographic fracture resulted on clearly defined (111) planes.

Tests were conducted at 10^{-6} torr to access the role of environment on the fatigue crack growth and to understand the micro-mechanisms of such failure. In our earlier study of a polycrystalline nickel-base superalloy, described in Section 3.4.1, the environment (laboratory air)

78

was found to be responsible for accelerated crack growth, possibly as a result of grain boundary weakening. In the case of single crystals, although such weakening sites are absent, it is yet to be seen if the subgrain, dendrites, inclusions, etc., would play a similar role. A detailed microstructural analysis of the fracture surface was conducted both under SEM and TEM for a better understanding of the micro-mechanisms of elevated temperature failure. Details of this investigation are available in Reference 23.

3.4.5   Hot Corrosion

Tests were conducted on 0.1-inch-thick precracked IN718 wedge open loaded specimens. The specimens were precracked in air and immersed in a molten pool of low melting point salt mixture of $NaNO_3$ + KNO_3, under static loading conditions. Several attempts were made to conduct CCG tests with specimens under a molten salt environment. In almost all cases, the furnace box corroded and failed due to long term exposure.

3.4.6   Creep Tests on Salt Coated Specimens

Creep rupture tests were conducted on IN718 tensile specimens at 800C. The specimen was coated with a salt mixture of 90% Na_2SO_4 + 10% NaCl. Tests were conducted

79

at 15, 20, and 30 ksi with both salt coated and uncoated specimens. The effect of salt degradation was pronounced at higher stresses [24].

3.4.7   Hot Corrosion Tests on Rene' 77 and Rene' 80

Hot corrosion tests were conducted on standard corrosion pins of Rene' 77 and Rene' 80. The pins were tested at 900C for 72 hours. The first batch of specimens were tested just for high temperature oxidation (with no salt). In the other two cases, the pins were spray coated with Na_2SO_4 and 90% Na_2SO_4 + 10% NaCl. No significant difference was noted in the hot corrosion behavior of Rene' 77 and Rene' 80. Detailed metallography was conducted on these specimens, which is discussed in Reference 24.

3.5   THRESHOLD BEHAVIOR

The evaluation of crack growth behavior in materials used in gas turbine engines has indicated the existence of both cycle-dependent and time-dependent effects. In determining the life of critical components, both types of effects and their interaction must be taken into consideration in a model. It has been shown that the stress intensity factor is an important parameter in characterizing both the cycle- and the time-dependent behavior in a life-prediction

model. Since a major portion of life is spent at the low growth rates, the behavior of the material must be well understood in this near-threshold regime. Because the crack growth behavior can be time-dependent, the load history and the frequency affect the near-threshold response.

An experimental program was initiated to evaluate the effects of frequency and hold-time on the near-threshold crack growth behavior of Inconel 718 at 649C in laboratory air. A test matrix was set up to evaluate the effect of frequencies from 0.01 to 30 Hz and of hold-times at maximum load up to 50 s. C(T) specimens are being tested using a computer controlled test machine. Closure loads are being evaluated from digitally acquired load-displacement or load-strain data.

3.6   MODELING CRACK GROWTH BEHAVIOR

3.6.1   Creep/Fatigue Interaction

An experimental investigation was conducted to evaluate the crack growth rates in Inconel 718 at 649C under symmetric and unsymmetric triangular waveshapes and triangular waves with hold-times at maximum load. The data have shown that the loading portion of a cycle was the major contributor to the time-dependent crack growth behavior. At low unloading frequencies or high load ratios, however, the

unloading portion of the cycle was found to become increasingly important. An analytical model was developed which predicts crack growth rate from an integration of the sustained load crack growth rates over the cycle when time-dependent behavior is dominant. Details of this study are discussed in Reference 15.

3.6.2 Crack Growth Variability at High Temperature

Fatigue crack growth rate, FCGR, tests were conducted at various K levels under computer control. Crack length values which were used to determine the K level and subsequent FCGR were obtained from measurement of compliance. The variability of resulting FCGR due to variability in crack length evaluation was studied as a function of frequency, temperature, and K. The experimental data did not show any trend in variability in FCGR as a function of temperature or frequency in the central power law region. Mean values of crack growth rates that were obtained from a least square fit of data within crack growth increments of 0.010, 0.015, 0.020, and 0.030 inch did not differ appreciably. This work was presented at the 1983 AIAA Mini-Symposium [25].

SECTION 4

ANALYTICAL INVESTIGATIONS

Conventional analytical and numerical methods were used to model the crack growth behavior of several turbine disc and blade alloys studied under experimental investigations. A variety of modeling techniques were utilized. Various computer programs were also written to minimize the time spent by the operator in setting up the input and to improve the results of the several finite element programs.

4.1 CONSTITUTIVE MODEL FOR THE POROUS PROCESS ZONE

It is fairly well established that subcritical crack extension under high temperature creep loading conditions occurs due to cavity nucleation and growth. The material in the crack tip process zone degrades due to cavitation. To characterize creep crack extension behavior, it is important to include the effects of cavities on the strength of the material.

The constitutive models for describing the solid matrix materials are well developed. One such model by Bodner and Partom [26] was applied for the characterization of a high temperature nickel-base alloy. To introduce the cavitation effect into the Bodner-Partom model, a simple methodology was

83

developed. Effects of void nucleation and growth were introduced through a pressure dependent yield criterion for materials containing voids. When this yield criterion is combined with the state variable flow theory of Bodner and Partom, the model was capable of calculating the reduced strength in the process zone due to cavitation. The developed constitutive model has void volume content as a continuum variable and thus, this parameter can be explored in the formulation for crack extension under creep loading conditions. Further discussion of the model is given in Reference 27.

4.2   UNIAXIAL CYCLIC STRESS-STRAIN CURVE USING BODNER-PARTOM
      CONSTITUTIVE MODEL UNDER ISOTROPIC/ANISOTROPIC FLOW
      CONDITIONS

A user-friendly interactive computer program called "BPANISO" was developed to solve the Bodner-Partom constitutive equations [28] under both isotropic and anisotropic material flow conditions. The equations are

$$\dot{\varepsilon}^{P} = \frac{2}{\sqrt{3}} D_0 e^{-(\frac{n+1}{2n})(Z/\sigma)^{2n}} , \qquad (6)$$

$$\dot{Z}^{+} = [Q+(1-Q)\frac{\sigma}{|\sigma|}]\dot{Z} \quad \text{for tension,} \qquad (7)$$

84

$$\dot{Z}^- = [Q-(1-Q)\frac{\sigma}{|\sigma|}]\dot{Z} \quad \text{for compression,} \tag{8}$$

$$\dot{Z} = m \ (Z_1-Z)\dot{W}_P-AZ_1(\frac{Z-Z_2}{Z_1})^r \ , \tag{9}$$

$$\dot{W}_P = \sigma\dot{\varepsilon}^P \ , \tag{10}$$

where $\dot{\varepsilon}^P$ is the uniaxial plastic strain rate, σ is the uniaxial stress, and Z is the state variable. The constants -- m, n, A, r, Z_1, and D_0 -- are model parameters. Q is the parameter that describes material flow condition with respect to the loading direction. Q = 1 implies that the flow is isotropic and Q = 0 implies that the flow is fully anisotropic. Any value between 0 and 1 indicates the level of anisotropy that is present in the material.

The values of Z in tension and compression were continuously calculated from Equations (7) and (8). However, the value of Z that appears in Equation (6) takes either Z^+ or Z^-, depending on the direction of the loading vector ($\sigma/|\sigma|$).

The solution time step in the program was automatically selected. An efficient and stable time stepping scheme was incorporated into the program. The time step was either increased or decreased, depending on the loading cycle. It

was reduced during a cycle when the plastic flow occurred and also when the rate changed its sign. The step size was increased during the elastic loadings and unloadings. The program could be used to simulate both strain and stress controlled cycles.

The BPANISO program, which was developed by Dr. A. M. Rajendran, was used in the investigation of several interesting solution cases and in a parametric study of the constants of the Bodner-Partom model by Beaman [29].

4.3   EFFECTS OF FINITE ELEMENT MESH ON THE STRESS INTENSITY
      FACTOR ANALYSIS OF SINGLE EDGE NOTCH SPECIMEN

In the application of finite element methods, one of the tasks for any user is the development of the mesh formulation. A mesh pattern must be carefully chosen so that reasonably accurate results are obtained. In the course of finite element application to solve problems in fracture mechanics, several interesting observations were made on the effect of various types of mesh patterns on the results for a single edge notch specimen. Solutions were obtained for various mesh formulations through two different finite element codes. The selected codes for this purpose were the general purpose, materially and geometrically nonlinear code 'MAGNA' [30] and the linear elastic code which will be referred to as the JA code [31].

The results obtained from the MAGNA code indicated that the following aspects are important for obtaining accurate results:

1. Very fine crack tip elements,

2. Evenly distributed nodes along a line of symmetry,

3. Uniform elements throughout the region away from the crack tip,

4. Reasonable number of nodes through which the loads were applied, and

5. Uniform distribution of degrees of freedom and elements throughout the geometry.

The stress intensity factor and crack opening displacement obtained from the mesh which was formulated based on the above aspects compared well within one percent to other analytical results.

The finite element mesh for the JA code contained special crack tip elements (with quarter point nodes) which simulated the theoretically suggested $\sqrt{r}$ singularity. The results indicated that even with very coarse elements away from the crack tip region, the stress intensity factor was determined with less than a 1% error. It was also observed that evenly distributed eight quarter point node elements around the crack tip yielded more accurate values for K than

the meshes with less than eight elements. In the runs using the JA code without the special crack tip elements, the accuracy of the results again very much depended on the mesh. The mesh that was formulated, based on the various aspects mentioned earlier, provided accurate results in the case of JA code also. The results of this investigation will be reported in a forthcoming technical report.

4.4   FINITE ELEMENT PROGRAM ENHANCEMENTS

Various computer programs have been written to minimize the time spent by the operator in setting up the input conditions and to expand the capability of evaluating parameters.

4.4.1   Preprocessor for 2D JA Program

Input file preparation for a finite element run is, in general, time consuming. To minimize the time involved in developing input data for:

1. A mesh for SE(T) and M(T) specimens,

2. Boundary conditions,

3. Applied loading conditions,

4. Options such as plane stress, plane strain, solution techniques, etc., and

5. Material properties,

a preprocessor program for the JA code [31] was developed. It is an interactive computer program. The unformatted data, entered interactively, is formatted according to the code requirements. The output file which is generated is the input file required to run the JA code. This newly developed preprocessor has significantly increased the efficiency when setting up the JA finite element program.

### 4.4.2 Mesh Generator Program for a Cracked Ring Specimen

The finite element mesh formulation for a geometry containing a crack is generally complex. The crack tip elements have to be fine while the elements in the zone away from the crack or the tip may be coarse. Significant time and effort is needed for generating a mesh pattern. When triangular elements are considered (as in VISCO [32] code), a large number of elements are needed to model the specimen accurately. Then, it is essential to generate the mesh pattern with an automatic mesh generator computer program. Any variation in the mesh pattern can be accommodated by easily modifying some portion of the main program. With these aspects included, a mesh generator program was developed and various mesh patterns were generated for a ring specimen. For the developed mesh, nodal coordinates and the corresponding element connectivities were obtained from this program.

### 4.4.3   J-Integral Routines in VISCO Computer Code

The special purpose finite element code
VISCO [32] was capable of calculating the J-integral parameter
only for paths which were parallel to cartesian coordinate
axes. Unfortunately, for a configuration such as a ring, the
J-integral paths in the mesh were not parallel to the axes.
In that case, the VISCO code could not provide the J-integral
calculations. To evaluate the J-integral for an appropriate
path using the VISCO code, additional routines were developed.

4.5   EFFECTS OF SIZE AND GEOMETRY ON NONLINEAR CORRELATION
PARAMETERS FOR CRACK BEHAVIOR

A finite element analysis (FEA) of cracked specimens
such as M(T) and SE(T) specimens was carried out to evaluate
the effects of geometry and size on nonlinear crack growth
parameters. Small and large sizes of M(T) and SE(T) specimens,
as shown in Figure 16, were selected. The corresponding
finite element meshes plotted on an equivalent scale are
shown in Figures 17 and 18. The crack tip elements for both
large and small specimens were identical. Mostly four node
isoparametric elements were used in these meshes. A few
triangular elements can be found among the crack tip elements.
The number of nodes, elements, and degrees of freedom for these
meshes are also shown in Figures 17 and 18.
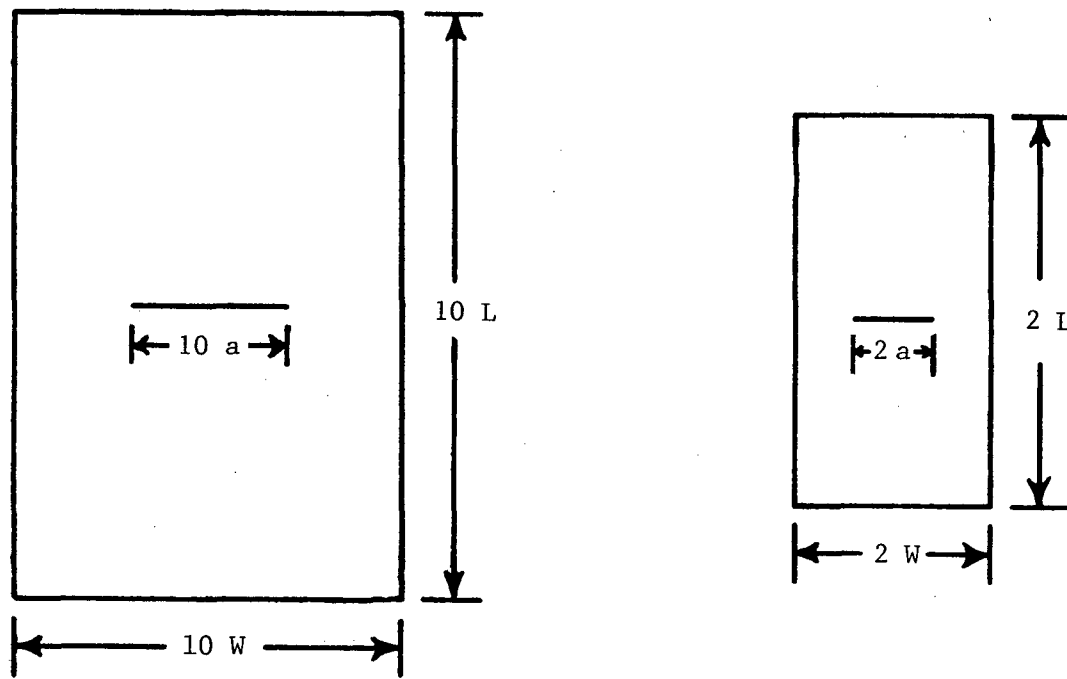
(a)
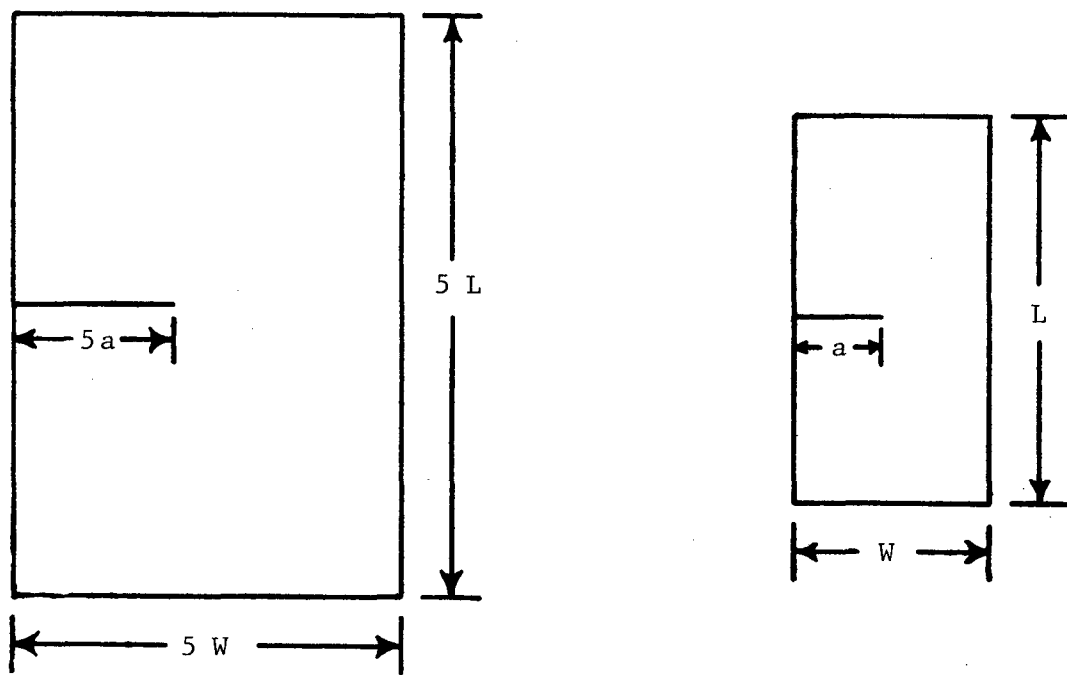
(b)

Figure 16. The Relative Specimen Sizes for (a) the CCT and
(b) the SEN Specimens.

91

LARGE CCT SPECIMEN

600 NODES
554 ELEMENTS
1147 DEGREES OF FREEDOM
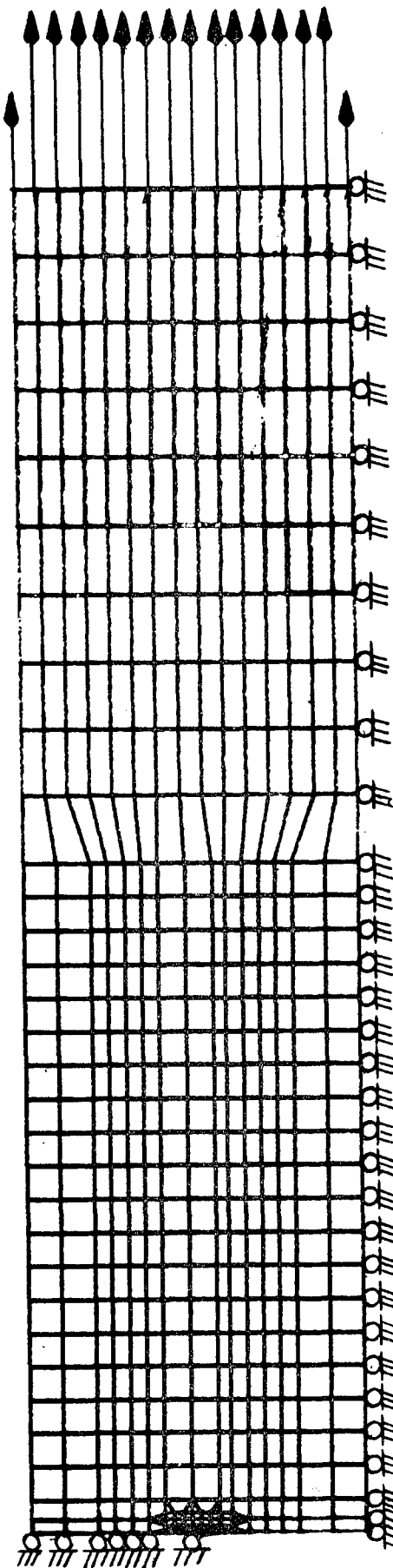
SMALL CCT SPECIMEN

160 NODES
138 ELEMENTS
292 DEGREES OF FREEDOM
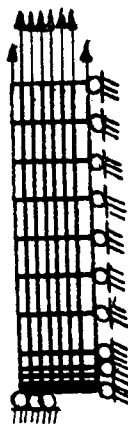
Figure 17. Meshes for the Small and Large Sizes of the CCT Specimen.

LARGE SEN SPECIMEN

400 NODES
404 ELEMENTS
858 DEGREES OF FREEDOM
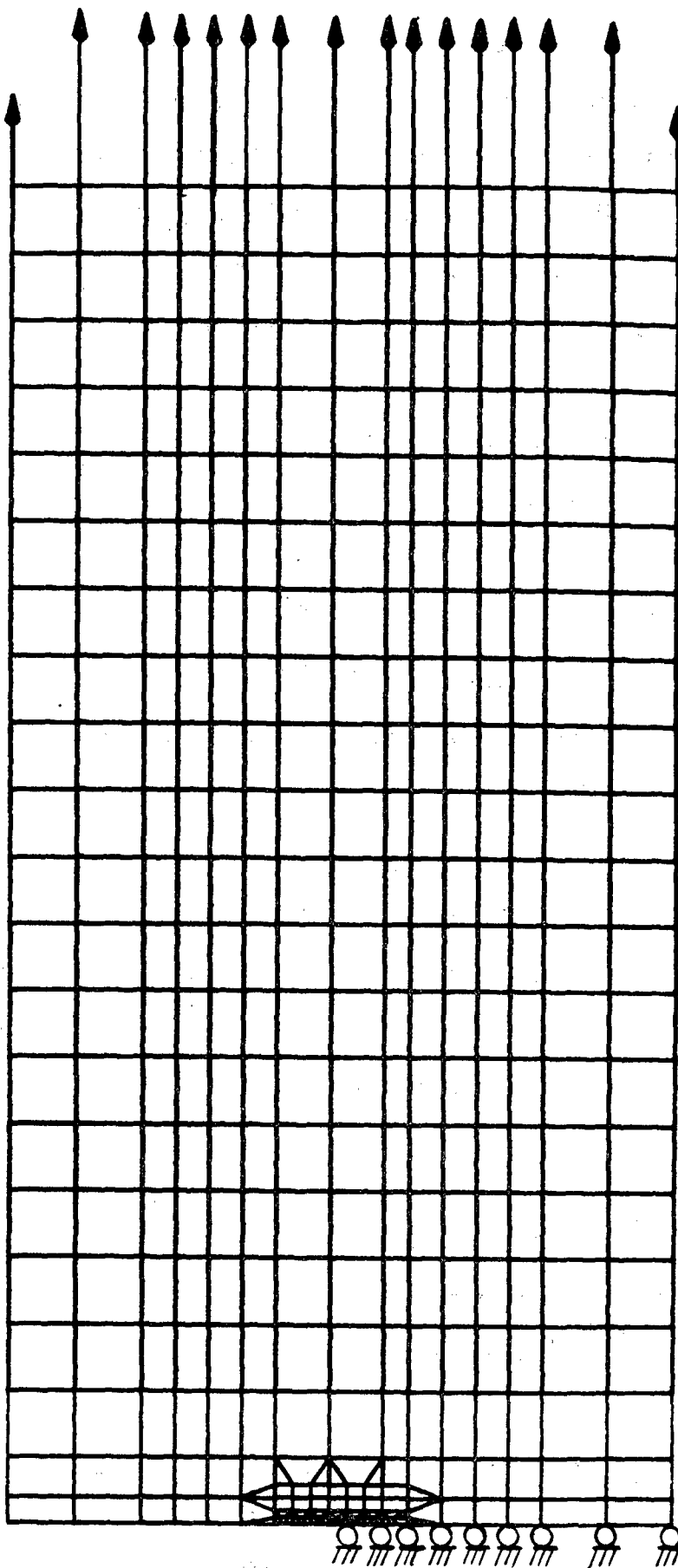
SMALL SEN SPECIMEN

128 NODES
110 ELEMENTS
240 DEGREES OF FREEDOM
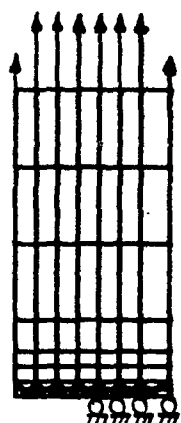
Figure 18. Meshes for the Small and Large Sizes of the SEN Specimens.

The SNAP finite element program, described in Section 4.7, was used in the FEA of various specimen geometries. For the analysis, the actual sizes of the specimens shown in Figure 16, are given by W = 1 in., a = 0.5 in., and L = 4 in. and all thicknesses were 1 in. The J-integral was calculated for various paths that transverse the crack counter-clockwise.

The nonlinear fracture parameters considered for the present study were:

a. The normalized effective stress intensity factor,

$K^* \equiv K_{eff}/(\sigma_Y \sqrt{W})$, and

b. The normalized plastic load-line displacement,

$\bar{V} \equiv \Delta V_p/V_e$,

where σ_Y is the initial yield stress, W is the width, ΔV_p is the plastic displacement, and V_e is the elastic displacement. K_{eff} is calculated from the elastic-plastic J-integral, J, from the following relationships:

$$K_{eff} = \sqrt{JE} \qquad \text{for plane stress,}$$

or

$$K_{eff} = \sqrt{\frac{JE}{1-\nu^2}} \qquad \text{for plane strain,}$$

where E is Young's modulus and ν is Poisson's ratio.

94

Experimental results [33] have been presented using plastic flow curves of K* versus $\overline{V}$ which represent the effect of the growth of crack tip plastic zone on the displacement during the loading of a precracked body. The plastic flow curve incorporates the effects of load level, flow property, aspect ratio, size and geometry on the resultant displacement due to the growth of the plastic zone.

To evaluate the size effects on the plastic flow curves, several computer runs were made under plane stress and plane strain conditions for large and small M(T) and SE(T) specimens with a/W = 0.5, E = 30 Mpsi, and σ_Y = 50 ksi as baseline values. The results are shown in Figures 19 and 20. It can be seen that there was insignificant difference in the plastic flow curves due to the size of the specimens for a given geometry. Both plane stress and plane strain conditions showed similar behavior. However, the plastic flow curves were different for different geometries. Based on these results, the size effect on the correlation parameters K* and $\overline{V}$ calculations was assumed to be negligible.

The influence of elastic modulus, E, and the yield stress, σ_Y, on the plastic flow curves were considered. Since effects of specimen size on the plastic flow curve was negligible, results were obtained only for the small specimen. Additional computer runs were made for M(T) and SE(T) specimens
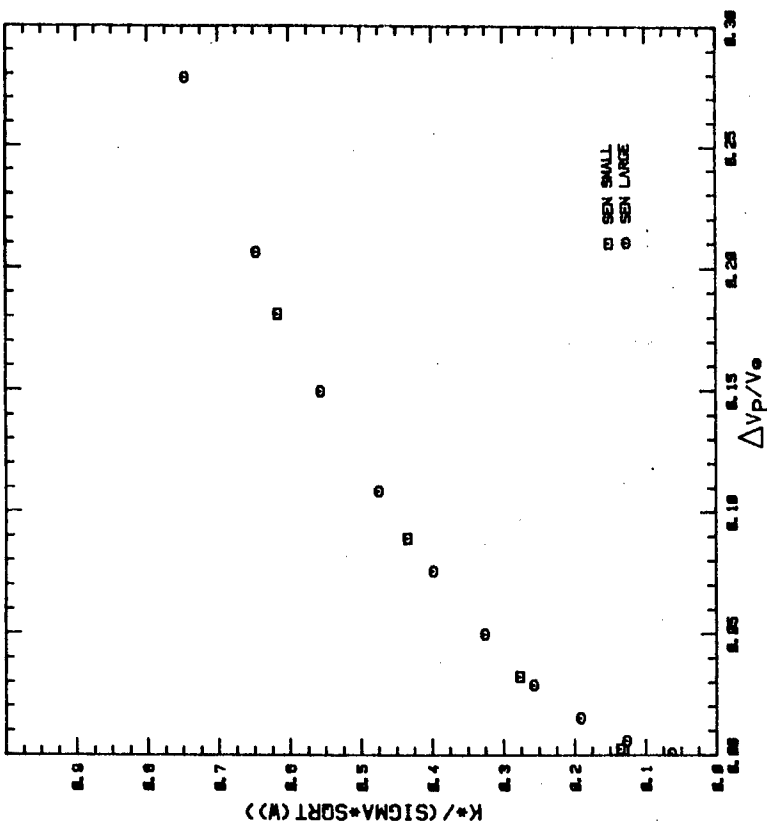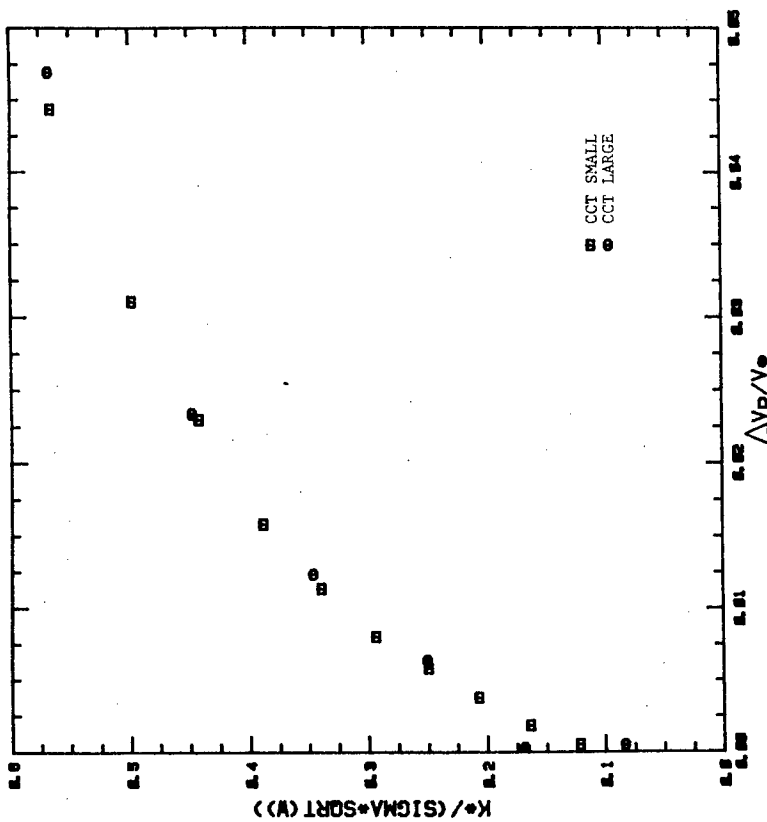
Figure 19. Size Effects on the Plastic Flow Curve Under Plane Stress Conditions for (a) CCT Specimens and (b) SEN Specimens.
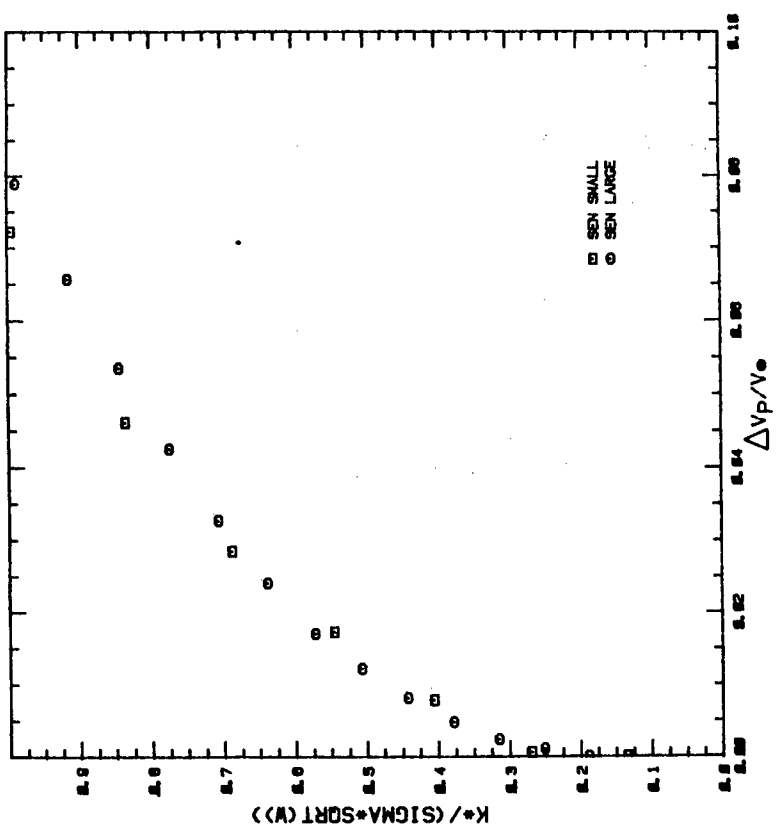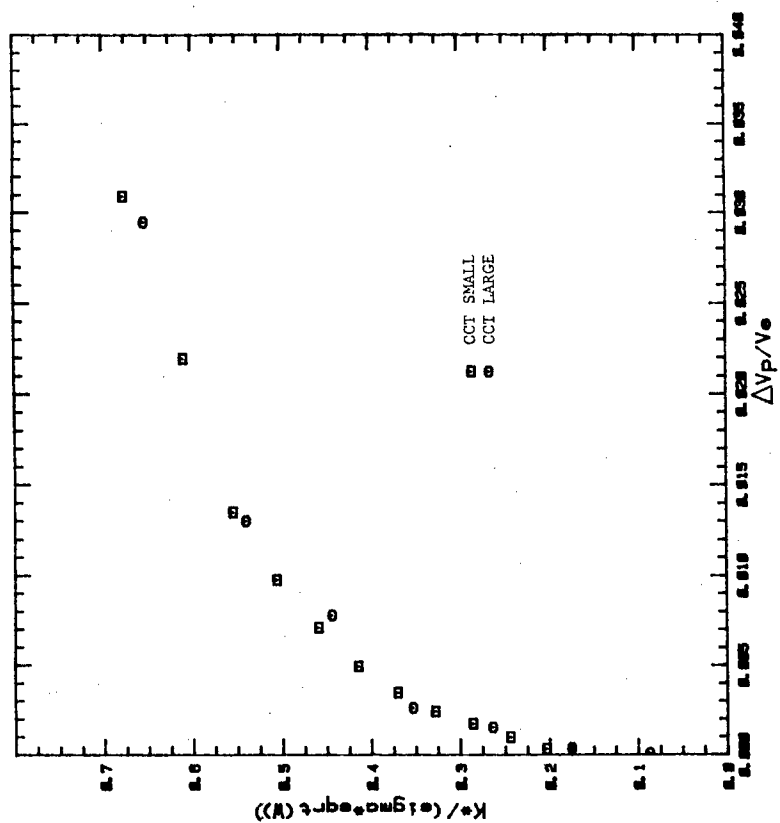
Figure 20. Size Effects on the Plastic Flow Curve Under Plane Strain
Conditions for (a) CCT Specimens and (b) SEN Specimens.

with σ_Y = 40 ksi. Both plane stress and plane strain
conditions were considered. The plastic flow curves were not
influenced by the material parameter, σ_Y, as can be seen from
Figure 21.

The influence of the elastic modulus was also
investigated. Several more computer runs were made on M(T)
and SE(T) specimens under both plane stress and plane strain
conditions for E = 20 Mpsi. The results are shown in Figure 22.
The plastic flow curves did not exhibit any strong dependency
on the elastic modulus.

For a/W = 0.5, the plastic zone size around the crack
tip of the large M(T) specimen was compared with the small
M(T) specimen under plane strain conditions. Zone sizes were
quite similar at lower stress intensity factors. Significant
differences occurred when the effective stress intensity
factor, K_{eff}, was greater than 30 ksi$\sqrt{in}$. For a K_{eff} = 30 ksi$\sqrt{in}$,
the plastic zone size of the small specimen was almost double the
size of the large specimen. Similar trends were observed under
plane stress conditions. The test results on compact tension
specimens [33] showed that as the width of a specimen increased,
the plastic zone size decreased.

Figure 21. Effect of Yield Stress, σ_Y, on the Plastic Flow Curve of Small CCT Specimens Under (a) Plane Stress Conditions and (b) Plane Strain Conditions.
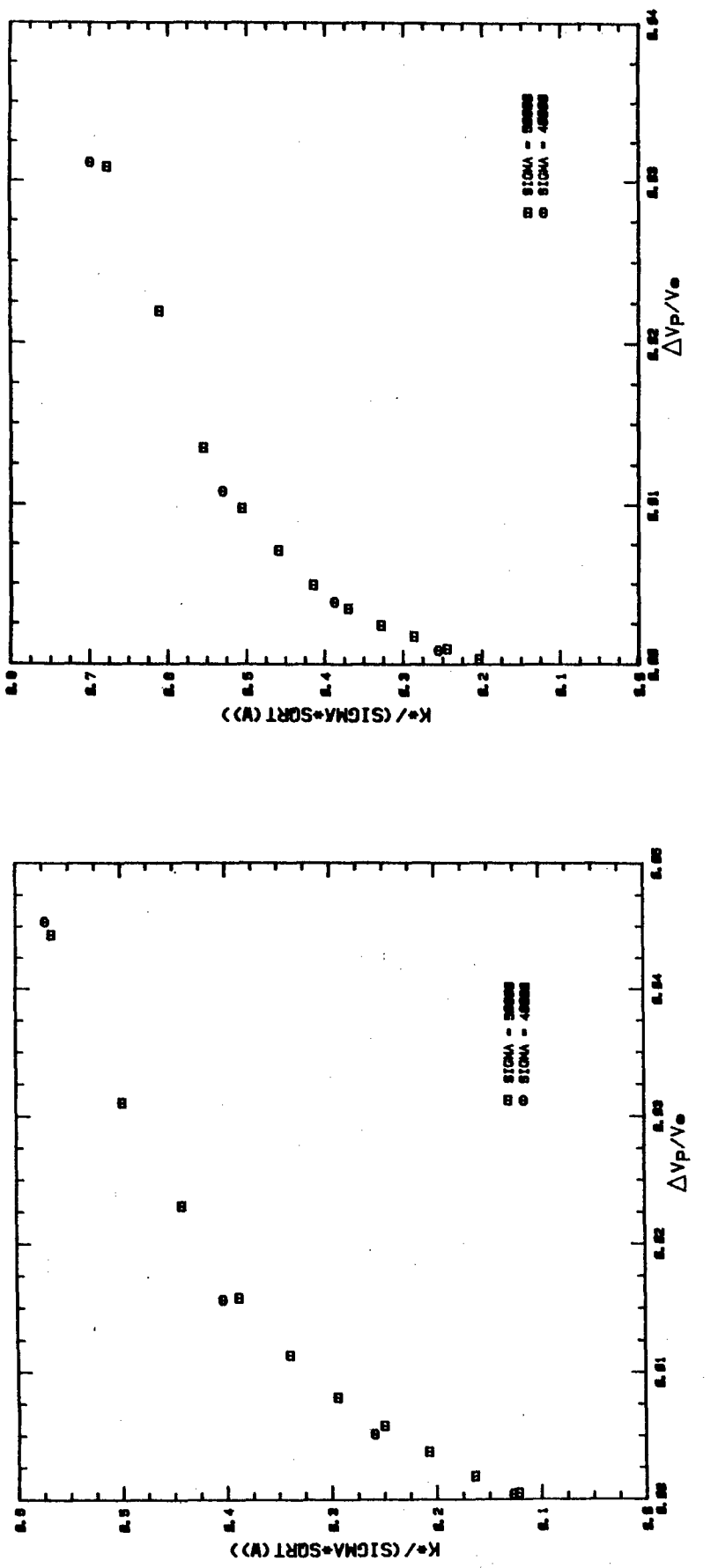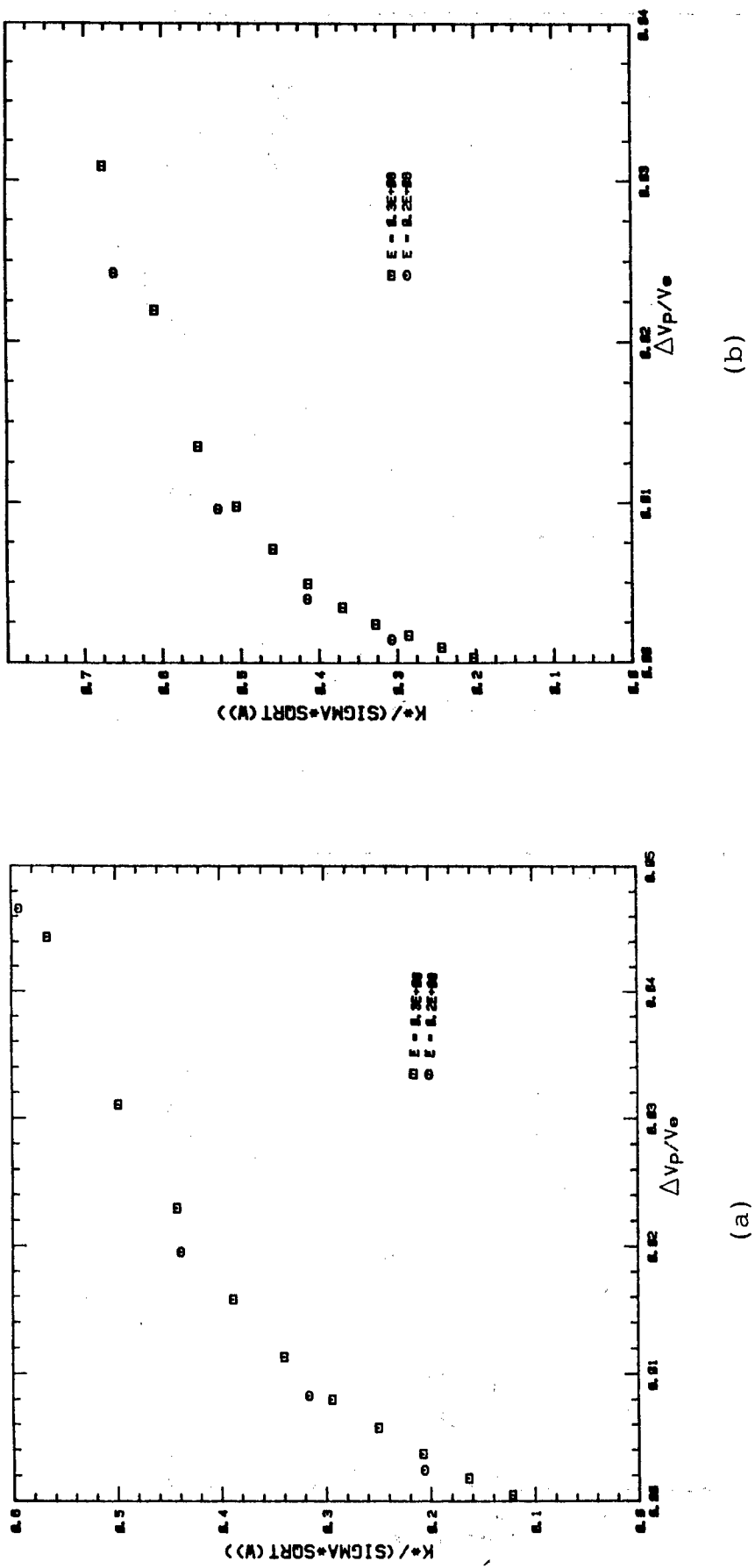
Figure 22. Effect of Modulus, E, on the Plastic Flow Curve of Small CCT Specimens Under (a) Plane Stress Conditions and (b) Plane Strain Conditions.

4.6   THREE DIMENSIONAL ANALYSIS OF CURVED CRACK FRONT

To provide additional insight into the crack growth
behavior under constant load, a three dimensional analysis of
a curved crack front was initiated using a code based on the
alternating finite element technique [34].   First, the analysis
of a nearly straight through-the-thickness crack was attempted.
The results did not agree with the results of the two
dimensional analysis for the same in-plane geometry.   It was
suspected that the input values for the code had not been
determined correctly.   To resolve the problem, input values
for a benchmark problem which had been analyzed and reported
in the literature were being determined.

4.7   SNAP PROGRAM FOR ANALYSIS OF CRACKED BODIES

SNAP (simple nonlinear analysis program) is a two
dimensional finite element analysis program [35] developed
for use in instruction and structural mechanics research.   The
code contained the necessary ingredients for rather
sophisticated treatment of nonlinear (large deformation,
plastic flow) structural problems, without the large element
library and elaborate data management functions typical of
larger finite element codes.

Several special purpose routines have been added to the basic SNAP program to analyze two dimensional geometries containing a crack. The routines included: (1) a path-independent integral (J-integral) calculation and (2) a node-release technique to simulate crack growth. Additional information on the modifications to SNAP and model problems that were used to validate the code are discussed in Reference 36.

4.8   STEADY STATE RESPONSE OF AN UNSUPPORTED RING

The aim was to calculate and analyze the steady state response of an unsupported ring for various forced frequencies. Since the applied point force was not symmetric, the entire ring specimen had to be modeled for the finite element analysis. A mesh generator program was developed for the full ring geometry. Using the preprocessor program, an input file was developed for the MAGNA code [31]. The finite element mesh, shown in Figure 23, contained 624 nodes, 192 elements, and 1,246 degrees of freedom. The finite element run was made for a two dimensional linear, elastic, plane stress problem. Since the degrees of freedom were too large, the computer runs were made only for three forced frequencies (1,000, 1,500, and 2,000 Hz). To analyze various loading and boundary conditions, it became essential to consider fewer degrees of freedom with fewer elements in the finite element formulation. For this purpose, a new mesh was formulated with very few degrees of freedom. The input file for MAGNA with the new mesh formulation is being developed.

X

Y

624 NODES
192 8 NODE QUAD

Psin(ωt)
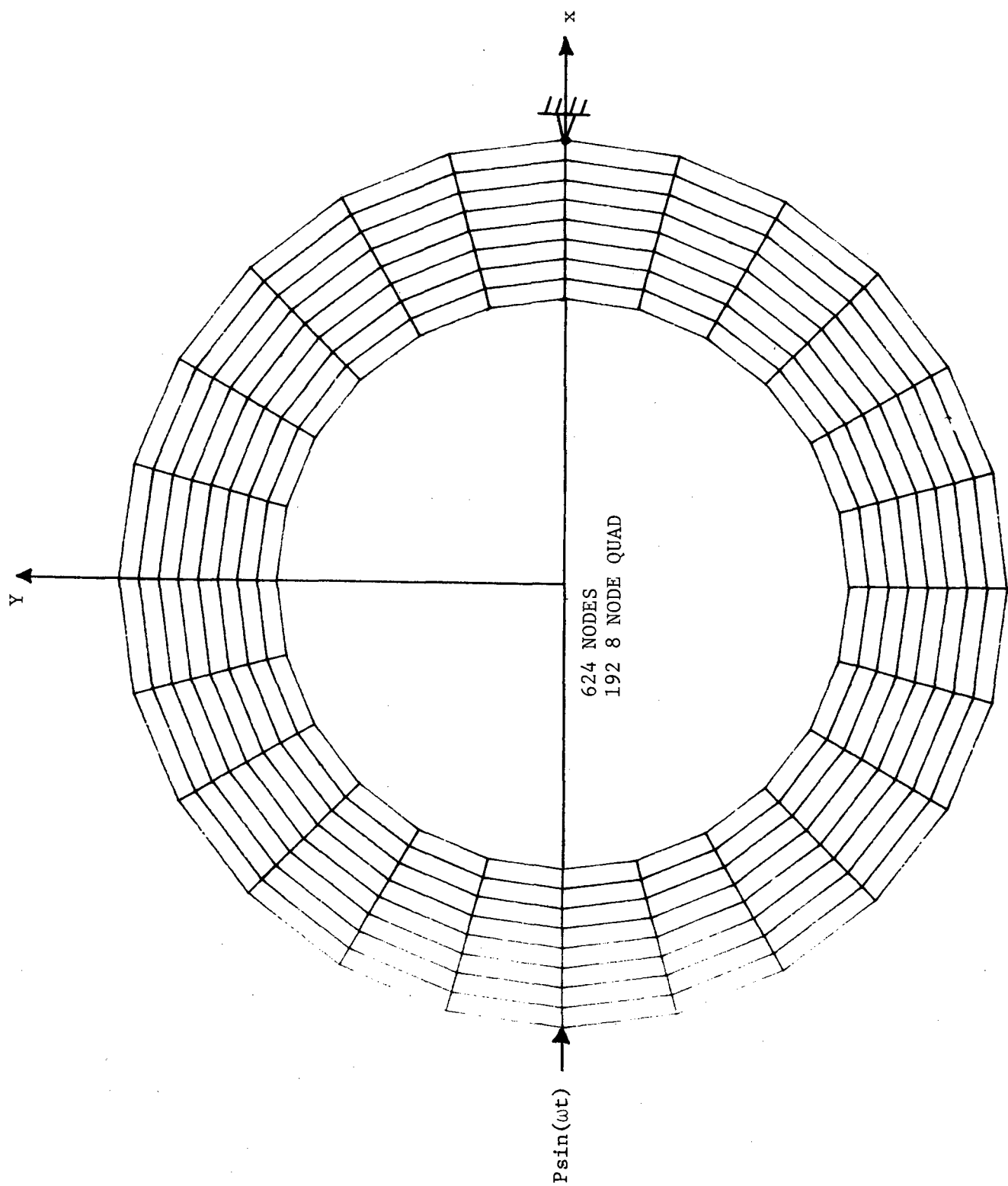
Figure 23. Finite Element Mesh for Dynamic Analysis of Ring.

SECTION 5

EVALUATION OF MECHANICAL PROPERTIES

Tests are conducted in the laboratory to provide basic
mechanical property data on existing and developmental materials.
The procedures set forth in ASTM Standard Test Methods are
followed for these tests unless otherwise directed by the
engineer/scientist. The tests include tensile, elastic modulus,
creep and creep rupture, low cycle fatigue, and high cycle
fatigue tests.

The types of tests that have been performed during the
contractual effort are fatigue crack growth at room temperature,
axial fatigue at room temperature and 455C, fracture toughness
at room temperature, and tensile tests from room temperature to
649C. These tests were performed on metal matrix composites
and various alloys of aluminum and titanium. After each test,
the data were analyzed, documented, and reported to the
respective project engineer.

The mechanical property data from these tests have been
used and are reported in the fourteen publications which are
listed in Appendix C.

SECTION 6

SUMMARY

A comprehensive multi-task research and development program was conducted to establish a sound life-prediction methodology for aircraft turbine disc and blade materials. The major emphasis was on the experimental investigations of crack growth behavior of these structural materials. A series of experiments dealing with fatigue crack growth behavior, creep crack growth behavior, creep/fatigue interaction, HCF/LCF behavior, environmental effects on creep/fatigue characteristics, and threshold behavior were conducted using state-of-the-art techniques.

During the course of the program, most of the existing experimental techniques were modified to obtain high quality data in the most efficient way. Generally, these modifications were achieved by the automation of most of the manually operated servo-hydraulic test systems and the introduction and implementation of sophisticated measurement techniques. Appropriate computer control systems were developed and successfully implemented. The test system automation and the hardware and software enhancements for a central data processing and archival system constituted one of the major efforts to provide a state-of-the-art experimental laboratory.

In this program, the electric potential technique was utilized as a more convenient way of determining crack length than optical measurements. Research was conducted on the application of compliance techniques to determine crack length and to evaluate the advantages of a particular technique in specific situations. An IDG rotating mirror IDG system which was used to resolve very small displacements for compliance measurements was interfaced with a PDP 11/24 computer which acquired and reduced data for short crack growth investigations. A laser interferometry system was developed to measure the interior opening of a surface crack in a transparent material.

In addition to the automation and upgrading of the laboratory systems, the experimental capability was expanded by designing and fabricating new systems to conduct thermal-mechanical fatigue tests and to enhance vacuum capability to study the effect of environment on elevated temperature creep/fatigue characteristics. An actuator system for the Theta Ring was designed for the study of HCF behavior and the automation of several HCF/LCF systems was also completed.

For the development of life-prediction methodology, the results of the experimental investigations were employed in the analytical modeling of crack growth behavior. As a result, models for the prediction of crack growth behavior were developed. The effect of frequency, stress ratio,

hold-time, and temperature on the crack growth behavior of IN718 was established. The influence of environment on crack growth behavior was quantified by test results, such as the crack growth rate of IN718 at 1200F in laboratory air was noted to be over an order of magnitude higher than in a vacuum environment of 10^{-6} torr.

In support of the experimental efforts, various analytical investigations were conducted which included the development of a constitutive model for a porous process zone, the evaluation of uniaxial cyclical stress-strain behavior using Bodner-Partom constitutive model, the effects of mesh analysis of SEN specimens, the enhancements to finite element program, the effects of size and geometry on nonlinear correlation parameters, the use of alternating method to analyze curved crack front in ring specimens, and the application of the SNAP program.

As part of the mechanical properties task, various tests such as uniaxial tension, compression, creep, fatigue, fatigue crack growth, etc., were conducted and the mechanical properties determined for a variety of structural materials including nickel-base superalloys and alloys of titanium and aluminum.

REFERENCES

1. Maxwell, D. C., Gallagher, J. P., and Ashbaugh, N. E.,
   "Evaluation of COD Compliance Determined Crack Growth
   Rates," AFWAL-TR-84-4062, Air Force Wright Aeronautical
   Laboratories, Wright-Patterson AFB, Ohio, June 1984.

2. Maxwell, D. C., "The Determination of Crack Length for
   Strain Measurement on a Compact Type Specimen," to be
   Published as an Air Force Wright Aeronautical Laboratories
   Technical Report, Wright-Patterson AFB, Ohio.

3. Nicholas, T., Ashbaugh, N. E., and Weerasooriya, T.,
   "On the Use of Compliance for Determining Crack Length in
   the Inelastic Range," Fracture Mechanics: Fifteenth
   Symposium, ASTM STP 833, R. J. Sanford, Ed., American
   Society for Testing and Materials, Philadelphia,
   Pennsylvania, 1984, pp. 682-698.

4. Ashbaugh, N. E., "Effect of Through-the-Thickness Stress
   Distribution Upon Crack Growth Behavior in a Nickel-Base
   Superalloy," Fracture Mechanics: Fourteenth Symposium -
   Volume II: Testing and Applications, ASTM STP 791,
   J. C. Lewis and G. Sines, Eds., American Society for
   Testing and Materials, 1983, pp. II-517-II-535.

5. Donath, R. C., Nicholas, T., and Fu, L. S., "An
   Experimental Investigation of Creep Crack Growth in IN100,"
   Fracture Mechanics: Thirteenth Symposium, ASTM STP 743,
   R. Roberts, Ed., American Society for Testing and Materials,
   1981, pp. 186-206.

6. Sharpe, W. N., Jr. and Martin, D. R., "An Optical Gage
   for Strain/Displacement Measurement at High Temperature
   Near Fatigue Crack Tips," Air Force Materials Laboratory,
   AFML-TR-77-153, Wright-Patterson AFB, Ohio, 1977.

7. Ashbaugh, N. E. and Ahrens, G. R., "Evaluation of Crack
   Closure," Presented at the AIAA 10th Annual Mini-Symposium
   on Aerospace Science and Technology, Air Force Institute
   of Technology, Wright-Patterson AFB, Ohio, 20 March 1984.

8. Wei, R. P. and Brazill, R. L., "An Assessment of AC and
   DC Potential Systems for Monitoring Fatigue Crack Growth,"
   Presented at an ASTM Symposium, Pittsburgh, Pennsylvania,
   October 1979.

9. Hartman, G. A., III, "A Thermal Control System for Thermal
   Cycling," Journal of Testing and Evaluation, JTEVA, Vol. 13,
   No. 5, September 1985, pp. 363-366.

10. Goodman, R. C. and Brown, A. M., "High Frequency Fatigue of Turbine Blade Materials," AFWAL-TR-82-4151, Air Force Wright Aeronautical Laboratories, Wright-Patterson AFB, Ohio, 1982.

11. Tait, R. W., "An Interferometric Approach to Evaluate Crack Closure in Transparent Specimens," Presented at the 11th Annual Mini-Symposium on Aerospace Science and Technology, Air Force Institute of Technology, Wright-Patterson AFB, Ohio, March 1985.

12. Tait, R. W., To be Published as an Air Force Wright Aeronautical Laboratories Technical Report, Wright-Patterson AFB, Ohio.

13. Jones, D. I. G., "Initial Design and Testing of a Unique High Frequency Fatigue Test System," to be Published in Shock and Vibration Bulletin, No. 55, 1985.

14. Weerasooriya, T. and Nicholas, T., "Hold-Time Effects in Elevated Temperature Fatigue Crack Propagation," AFWAL-TR-84-4184, Air Force Wright Aeronautical Laboratories, Wright-Patterson AFB, Ohio, March 1985.

15. Nicholas, T., Weerasooriya, T., and Ashbaugh, N. E., "A Model for Creep/Fatigue Interactions in Alloy 718," Fracture Mechanics: Sixteenth Symposium, ASTM STP 868, M. F. Kanninen and A. T. Hopper, Eds., American Society for Testing and Materials, Philadelphia, Pennsylvania, 1985, pp. 167-180.

16. Stucke, M. A. and Weerasooriya, T., "Observations on Micro-Mechanisms of Crack Growth as a Function of Temperature and Frequency," Presented at TMS-AIME Fall Meeting, Philadelphia, Pennsylvania, October 1983.

17. Brown, A. M., "Effect of High Cycle/Low Cycle Loads on the Crack Growth Behavior of Inconel-718," 9th Annual AIAA Mini-Symposium on Aerospace Science and Technology, Air Force Institute of Technology, Wright-Patterson AFB, Ohio, 22 March 1983.

18. Brown, A. M., "Major-Minor Cycle Crack Propagation Behavior of Alloy-718 at Elevated Temperature," Presented at the Sixteenth National Symposium on Fracture Mechanics, Battelle Columbus Laboratories, Columbus, Ohio, August 1983.

19. Brown, A. M. and Stucke, M. A., "Major/Minor Cycle Crack Propagation Behavior of Inconel-718 at Elevated Temperature," Presented at the TMS-AIME Fall Meeting, Philadelphia, Pennsylvania, October 1983.

20. Ramsey, S. W. and Ashbaugh, N. E., "A Model for HCF/LCF Crack Growth Behavior," Presented at 10th Annual Mini-Symposium on Aerospace Science and Technology, Air Force Institute of Technology, Wright-Patterson AFB, Ohio, March 1984.

21. Ashbaugh, N. E., "Effect of Through-the-Thickness Stress Distribution Upon Crack Growth Behavior in a Nickel-Base Superalloy," Fracture Mechanics: Fourteenth Symposium - Vol. II: Testing and Applications, ASTM STP 791, J. C. Lewis and G. Sines, Eds., American Society for Testing and Materials, 1983, pp. II-517-II-535.

22. Stucke, M., Khobaib, M., Majumdar, B., and Nicholas, T., "Environmental Aspects in Creep Crack Growth in Nickel-Base Superalloy," Advances in Fracture Research, Vol. 6, Sixth International Conference on Fracture, New Delhi, India, December 1984.

23. Venkataraman, S., Nicholas, T., and Khobaib, M., "Elevated Temperature Fatigue Crack Growth of Rene' N4 Single Crystals," Presented at and to be Published in the Proceedings of the TMS-AIME Fall Meeting, October 1985.

24. Balsone, S. J., "The Effect of Stress and Hot Corrosion on Nickel-Base Superalloys," to be Published as an M.S. Thesis at the Air Force Institute of Technology, Wright-Patterson AFB, Ohio.

25. Dirkes, E. M. and Weerasooriya, T., "Variability of Fatigue Crack Growth Rate as a Function of Temperature, Frequency, and Stress Intensity Factor for Constant K Testing," Presented at AIAA Mini-Symposium on Aerospace Science and Technology, Air Force Institute of Technology, Wright-Patterson AFB, Ohio, March 1983.

26. Bodner, S. R. and Partom, Y., "Constitutive Equations for Elastic-Viscoplastic Strain-Hardening Materials," Journal for Applied Mechanics, Vol. 42, 1975, pp. 385-389.

27. Rajendran, A. M., "Constitutive Models Based on Compressible Plastic Flaws," Proceedings of the NASA Conference on Nonlinear Constitutive Relations for High Temperature Applications, NASA CP-2271, 1983.

28. Bodner, S. R., Partom, I., and Partom, Y., "Uniaxial Cyclic Loading of Elastic-Viscoplastic Materials," ASME Journal of Applied Mechanics, Vol. 46, 1979, pp. 805-810.

29. Beaman, R. L., "The Determination of the Bodner Material Coefficients for IN718 and Their Effects on Cyclic Loading," MS Thesis, AFIT/GAE/AA/84M-1, Air Force Institute of Technology, Wright-Patterson AFB, Ohio, March 1984.

30. Brockman, R. A., "MAGNA: Finite Element Program for the Materially and Geometrically Nonlinear Analysis of Transient Loading," AFWAL-TR-80-3152, Air Force Wright Aeronautical Laboratories, Wright-Patterson AFB, Ohio, January 1981.

31. Ahmad, J., "Two Dimensional Linear Elastic Analysis of Fracture Specimens: User's Manual of a Finite Element Computer Program," Technical Report AFWAL-TR-80-4008, Air Force Wright Aeronautical Laboratories, Wright-Patterson AFB, Ohio, February 1980.

32. Hinnerichs, T., Nicholas, T., and Palazotto, A., "A Hybrid Experimental-Numerical Procedure for Determining Creep Crack Growth Rates," Engineering Fracture Mechanics, Vol. 6, 1982, pp. 265-277.

33. Banerjee, S., "Influence of Specimen Size and Configuration on the Plastic Zone Size, Toughness, and Crack Growth," Engineering Fracture Mechanics, Vol. 15, No. 3-1, pp. 343-390.

34. Smith, F. D. and Kullgren, T. E., "Theoretical and Experimental Analysis of Surface Crack Eminating from Fastener Holes," AFFDL-TR-76-104, Air Force Flight Dynamics Laboratory, Wright-Patterson AFB, Ohio, February 1977.

35. Brockman, R. A., "SNAP: A Simple Nonlinear Analysis Program for Education and Research," UDR-TM-82-06, University of Dayton Research Institute, Dayton, Ohio, February 1982.

36. Rajendran, A. M. and Brockman, R. A., "A Simple Nonlinear Analysis Program - Validation and Input Preparation," Submitted for a University of Dayton Research Institute Technical Report.

APPENDIX A

TEKTRONIX 4052 SYSTEM

APPENDIX A

TEKTRONIX 4052 SYSTEM

A block diagram of the control system is illustrated in
Figure A1. The functions of the equipment which is connected
on the IEEE-488 bus are described below.

- Printer - Prints the data samples.
- Cycle Counter - Counts the number of cycles by
  monitoring the load or function generator signal.
- Nicholet Digital Oscilloscope - Digitizes and displays
  load and displacement amplifier signals. The disk
  drive in the oscilloscope is used to store the load
  displacement waveform when high speed data acquisition
  is required. Compliance of the test specimen is
  computed from the digitized load displacement data.
  The ability to trigger at a given point of waveform
  reduces the software development time for complicated
  waveforms.
- HP Voltmeter - Acquires mean values of electric
  potential of the cracked specimen.
- HP Power Supply - Supplies a constant current of
  9.5A across the cracked specimen. The power supply
 is switched off by the computer in acquisition of
  thermal EMF.
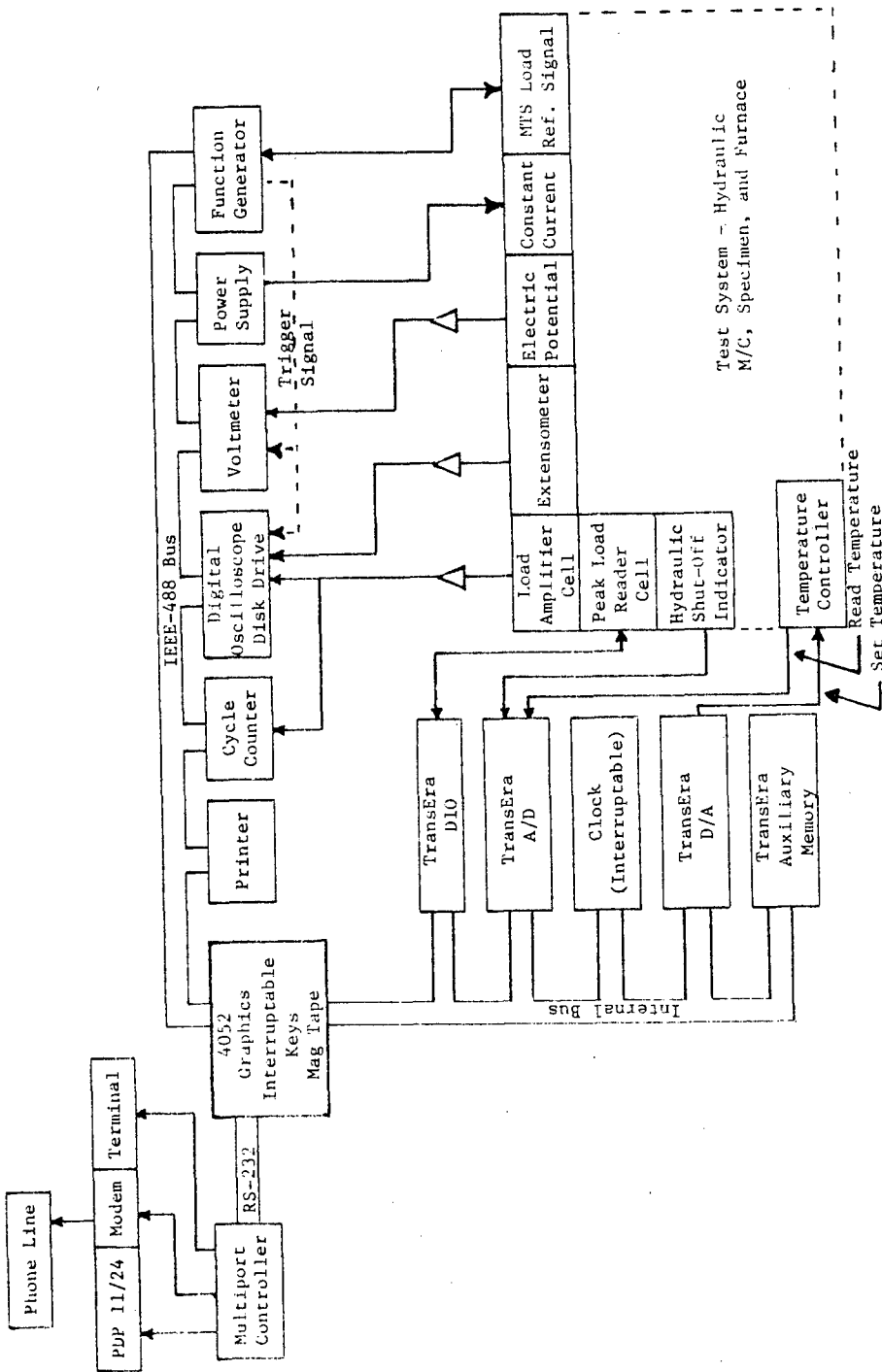
Figure Al. Block Diagram of Test System Hardware.

114

- Wavetek Function Generator – Provides the reference load signal to the hydraulic machine. By mixing the four programmed RAM waveforms and clock with interruptable capability, very complicated engine spectra can be created. A trigger signal can be obtained at predetermined positions of the waveforms.

The following instruments are connected to the Tektronix 4052 internal bus:

- Thirty-two Bit DIO Module with Handshaking – Resets and acquires peak reader values from the servo-hydraulic machine.
- Eight Channel A/D – Monitors the furnace temperature and status of the hydraulic machine. Monitoring of the cooling system will be added in the near future.
- Interruptable Clock – Stamps the time of the data samples. Interruptable capability is used in generation of hold-times for complicated waveforms.
- Two Channel D/A Module – Provides set point information for the furnace controller unit.
- Auxiliary Memory – Provides a RAM disk for temporary storage of data samples and programs.

A five channel multiport controller which uses switchable software is connected to the RS-232 port of the Tektronix 4052A.

The software provides control of the following: (a) HOST PDP 11/24 - Data transfer, reduction, and report quality graphics, and mass storage, (b) Modem Connected to a Phone Line - CDC or home monitoring and control of long term tests, and (c) Terminal - Monitoring of tests from office or any other desired place in the laboratory.

In addition, the 4052A is equipped with a high resolution graphics CRT and an internal tape drive storage unit. High resolution graphics display is used in monitoring real-time crack growth and growth rates graphically.

Software that has been developed is used for the following types of crack growth testing and modes of monitoring the tests:

- Decreasing stress intensity precracking (ASTM E399).
- Decreasing stress intensity threshold (exponential).
- Constant stress intensity testing.
- Constant load testing.
- Complicated waveform testing.
- Frequency shedding tests.
- Temperature shedding tests.
- Compliance and/or electric potential crack length monitoring based on the frequency condition.
- Test monitoring via phone/modem.
- Real-time data analysis and graphical display.

- Crack closure monitoring and display.

- Alarm shutdown.

APPENDIX B

PDP 11/24 SYSTEM FOR FATIGUE CRACK GROWTH

APPENDIX B

PDP 11/24 SYSTEM FOR FATIGUE CRACK GROWTH

A block diagram of the control system is illustrated in Figure B1. Subroutines had to be written to address hardware for automated test control and to support the software program. The following utility routines were written for the IEEE-488 card:

- ATT488 - Attaches IEEE-488 bus to the task.

- DET488 - Detaches IEEE-488 bus to the task.

- WTSRQ - Waits for an SRQ from the attached devices. Also identifies and gets the status of the device requesting the service.

- SEND88 - Sends a string of ASCII characters to the specified device.

- RECV88 - Receives a string of ASCII characters from a specified device.

The following library routines were written to support the main control program:

- ADSCAN - A single A/D sweep is made of an analog device attached to the LPA11. An array will contain the differential values from Channels 1 and 2.
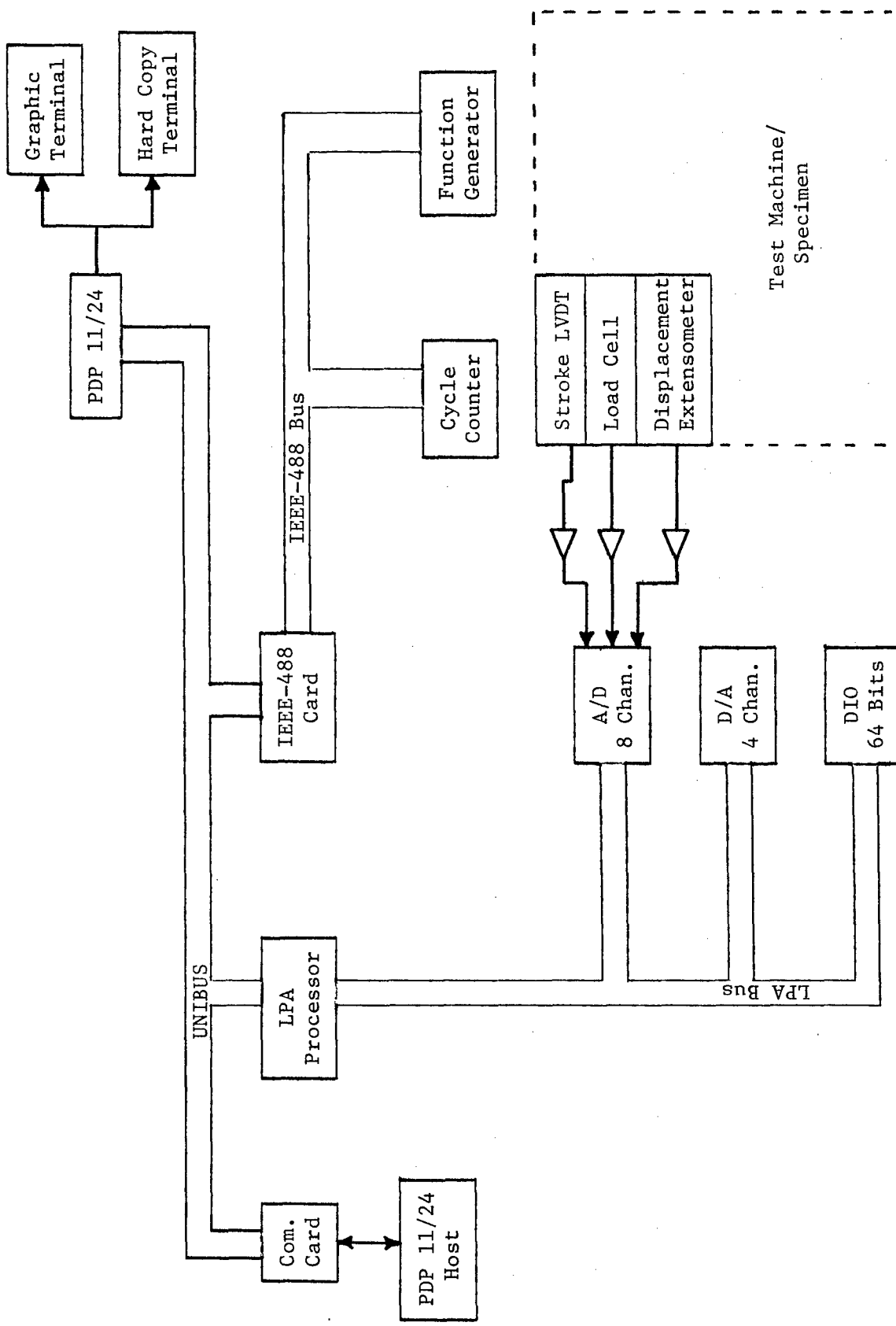
Figure B1. Hardware Configuration of PDP 11/24 Test System.

120

- ACOMP - Crack length is calculated for three different specimen geometries from the input compliance values.

- KCALC - Stress intensity factor is calculated for six specimen geometries.

- PCALC - Load is calculated for six different geometries for a given stress intensity.

- COMPLY - The A/D is scanned for load versus displacement data and compliance value is calculated for three different geometries. Also, maximum and minimum values of load and displacement information are outputs from this routine.

- INILPA - LPA11 processor is initialized for data acquisition.

- CUTAD - A/D input is converted to a floating point voltage number.

- XRATE - Clock parameters of LPA11 are calculated for a given sample rate.

- ADMXMN - A single A/D sweep is made on Channels 1 and 2 (differential). Maximum and minimum of Channel 1 and the values of Channel 2 which correspond to these maximum and minimum are determined.

- INIPRE - Calculates constants required for ASTM precracking procedure or linear precrack load shedding procedure.

APPENDIX C

LIST OF PUBLICATIONS REPORTING
MECHANICAL PROPERTY DATA

APPENDIX C

LIST OF PUBLICATIONS REPORTING
MECHANICAL PROPERTY DATA

Schwenker, S. W., Eylon, D., and Froes, F. H., "Performance Optimization in PM Titanium Components," Materials and Process In Continuing Innovations, Vol. 28, SAMPE, Covina, California, 1983, pp. 436-447.

Eylon, D., Froes, F. H., and Gardiner, R. W., "Developments in Titanium Alloy Casting Technology," Journal of Metals, Vol. 35, No. 2, 1983, pp. 35-47.

Vogt, R. G., Froes, F. H., Eylon, D., and Levin, L., "Thermo-Chemical Treatment (TCT) of Titanium Alloy Net Shapes," Titanium Net-Shape Technologies, Ed. by F. H. Froes and D. Eylon, TMS-AIME Publications, Warrendale, Pennsylvania, 1984, pp. 107-120.

Abkowitz, S., Kardys, G. J., Fujishiro, S., Froes, F. H., and Eylon, D., "Titanium Alloy Shapes from Elemental Blend Powder and Tensile and Fatigue Properties of Low Chloride Compositions," Titanium Net-Shape Technologies, Ed. by F. H. Froes and D. Eylon, TMS-AIME Publications, Warrendale, Pennsylvania, 1984, pp. 107-120.

Eylon, E., Froes, F. H., and Levin, L., "Effect of Hot Isostatic Pressing and Heat Treatment on Fatigue Properties of Ti-6Al-4V Castings," to be Published in the Proceedings of the 5th International Conference on Titanium, Munich, West Germany, 1984.

Mahajan, Y. R., Eylon, D., Kelto, C. A., Egerer, T., and Froes, F. H., "Modification of Titanium Powder Metallurgy Alloy Microstructures by Strain Energizing and Rapid Omni-Directional Compaction," to be Published in the Proceedings of the 5th International Conference on Titanium, Munich, West Germany, 1984.

Herteman, J. P., Eylon, D., and Froes, F. H., "Mechanical Properties of Advanced Titanium Powder Metallurgy Compacts," to be Published in the Proceedings of the 5th International Conference on Titanium, Munich, West Germany, 1984.

Boyer, R. R., Eylon, D., and Froes, F. H., "Comparative Evaluation of Ti-10V-2Fe-3Al Cast, P/M and Wrought Product Forms," to be Published in the Proceedings of the 5th International Conference on Titanium, Munich, West Germany, 1984.

Levin, L., Vogt, R. G., Eylon, D., and Froes, F. H., "Fatigue Resistance Improvement of Ti-6Al-4V by Thermo-Chemical Treatment," to be Published in the Proceedings of the 5th International Conference on Titanium, Munich, West Germany, 1984.

Weiss, I., Eylon, D., Toaz, M. W., and Froes, F. H., "Effect of Isothermal Foring on Microstructure and Fatigue Behavior of Blended Ti-6Al-4V Powder Compacts," Met. Trans. A, In Press, 1985.

Eylon, D., Schwenker, S. W., and Froes, F. H., "Thermally Induced Porosity in Ti-6Al-4V Prealloyed Powder Compacts," Met. Trans. A, In Press, 1985.

Schwenker, S. W., Eylon, D., and Froes, F. H., "Influence of Foreign Particles on Fatigue Behavior of Ti-6Al-4V Prealloyed Powder Compacts," Met. Trans. A, In Press, 1985.

Kirchoff, S. D., Young, R. H., Griffith, W. M., and Kim, Y. W., "Microstructural/Strength/Fatigue Crack Growth Relations in High Temperature P/M Aluminum Alloys," Proceedings of High Strength P/M Aluminum Alloys, Ed. by M. J. Koczak and G. J. Hildeman, 1982.

Smith, P. R., Froes, F. H., and Cammett, J. T., "Correlation of Fracture Characteristics and Mechanical Properties for Titanium Matrix Composites," AIME, Dallas, Texas, February 1982.